Author comment replying to the referee comments by F. Saito

We'd like to thank the reviewer their comments on the manuscript and would hereby like to address the concerns they raised. Comments in italics, below our rebuttal. Page and line numbers refer to the revised manuscript.

Abe-Ouchi et al (2013) use a different approach to force an ice-sheet model, in which a series of GCM snapshots are used to separate orbital, CO2, albedo etc effects on ice- sheet surface temperature. The method is not the same as two approaches (glacial index method and ESM coupling), and also not the same as the approach of the present paper. This study is limited to the northern hemisphere, but if the authors agree (I am not sure whether it is fair to tell this, because I am one of the authors of the paper), the authors may include the study as yet another example of hybrid GCM ice-sheet model application. In addition, several processes not included in the model are discussed in conclusion (around p13), which are discussed in Abe-Ouchi (2009, 2013).

We agree that this is a very interesting and relevant study and will include a reference to it in the Introduction and Conclusions sections of our manuscript.

P2, L27: Added a reference to the work by Abe-Ouchi et al. (2013).

P14, L27: Added a few lines discussing the results reported by Abe-Ouchi et al. (2013).

As far as I understand, since ice sheet evolution is computed on the four separate regions, there is no chance to connect two ice sheets, e.g., Greenland and North America. In Fig. 4 the northwest part of Greenland seems to connect with NA ice sheet. I wonder how to handle this situation.

It is true that the Greenland and Laurentide ice-sheets cannot connect in our model – in the North America module, the bedrock of Greenland has been manually lowered to well below sea-level, and vice versa in the Greenland module. This was done first by de Boer et al. (2013) to enable them to run the Greenland module at a higher resolution and more importantly with a mass balance module dedicated specifically for Greenland and one for the North America module. The large-scale behaviour of the two ice-sheets in terms of sea-level contribution, which is the main focus of our model, is not significantly affected by this and so we decided not to change this in our model version.

Moreover, also in Fig. 4 or 7, simulated NA ice sheet extends on Eurasia. How to treat this? I suspect the model domain of NA ice sheet cover until East Siberia. Of course it is reasonable to assume that Siberia has been ice-free, in principle this is just an specification of the model of this paper. It is better to clarify these configuration. Possibly, it is enough to describe the four separated domain on the map.

Although this is not mentioned in the text, Figure 5 is the North America grid of the model. It does indeed cover the entire Bering Strait, as well as a very small portion of north-east Siberia. Since that area of the world is very dry, none of our simulations have ever encountered ice at the edge of the model grid. We will refer to a figure of the grid as presented in Fig. 3 in de Boer et al. (2014) which displays the same grid as used here.

P5, L10: Added a reference to the relevant figure from de Boer et al. (2014).

p1 L10 'all ice' it too much. as far as I understand, neither glacier nor sea ice is included.

We agree that this statement is incorrect. We will correct this in the manuscript.

P1, L10: changed the statement to correctly describe what ice is simulated by the model: "…thermodynamic ice-sheet-shelf model calculating the four large continental ice-sheets (Antarctica, Greenland, North America and Eurasia), …"

p3 L5 LGM should be defined here (now defined at L29).

We agree, and will correct this in the manuscript.

P3, L24: Added the definition of LGM

P4, L16: Removed the definition of LGM

p4 L4 degree C should be K.

We agree, and will correct this in the manuscript.

P4, L22: Changed degree C to K.

p14 Eq A4, etc. write '\exp' instead of 'exp' if using LaTeX.

We agree, and will correct this in the manuscript.

P16, L17 (Eq. A5): Changed "$\exp^{(\cdots)}$" to "$e^{(\cdots)}$".

p15 L1. 2e-11, etc, should be written as 2 \times 10^{-11}.

We agree, and will correct this in the manuscript.

P16: Corrected all exponents.

p15 L25 refer Table 1 after c3.

We agree, and will correct this in the manuscript.

P17, L25: Added a reference to Table 1 for values of parameter c3.

Fig.1. Need to describe the color as bedrock elevation where not covered by ice.

Fig.5,8,9. Need to describe the contour lines (thickness or surface elevation?)

We agree, and will add this information to the figure captions.

Fig. 1, 4, 5, 7, 8, 9: Added description of the colormap and contour lines to the figure captions.

Author comment replying to the referee comments by L. Tarasov and T. Bahadory

We'd like to thank the reviewers for their comments on the manuscript and would hereby like to address the concerns they raised.

The reviewers raised several questions about technical aspects of the model set-up presented in the manuscript, especially regarding the rationale behind the choices of different parameterisations. We agree that the manuscript could be improved at this point and we clarified this in the new version, details are listed below.

We'd like in particular to express our gratitude to the reviewers for pointing out an important detail – the fact that the stated dimensions of some of the parameters in the precipitation model were erroneous had indeed escaped our attention.

In Italics the comments, below our rebuttal. Page and line numbers refer to the revised manuscript.

The inclusion of "GCM" in the title is misleading.

We agree that the current title could be interpreted as meaning we constructed a coupled GCM-ISM. We will change the title to more accurately reflect our model set-up, where an ISM is forced with output from a GCM.

P1, L1: changed the manuscript title.

with pre-calculated output from
several steady-state simulations with the HadCM3 general circulation model
 # Inaccurate and misleading. Two simulations is not "several".

Although the method presented in this manuscript can be used to force the ice-sheet model with output from any number of GCM snapshots, the results presented here were indeed produced with only two snapshots. We agree that the statement is inaccurate, and will correct this.

P1, L11: changed "several" to "two".

P1, L16: clarified that the presented method can be applied to a matrix containing any number of GCM snapshots.

The simulated ice-sheets at LGM agree well with the ICE-5G
reconstruction and the more recent DATED-1 reconstruction in terms of
total volume and geographical 20 location of the ice sheets.
 # Since ICE-5G use DATED-1 precursors for margin constraint and
 # since the GCM was forced with ICE-5G boundary conditions, this

 # is a weak result

pg 10 comparison to ICE5-G
 # GCM fields generated with say ICE5-G boundary conditions will have a
 # strong imprint of the ice sheet margin on the resultant climate. So
 # recreating ICE5-G ice extent with this interpolated climate forcing
 # offers little validation as to the utility of the approach. For me,
 # the challenge is to get a range of climates without the imprint of
 # assumed ice sheet boundary conditions used by the GCM.

As is shown in the referenced study by Niu et al. (2017), forcing a GCM with a certain prescribed ice-sheet and then using the resulting climate to force an ice-sheet model is by no means a guarantee that that ice-sheet model will produce the same ice-sheet that was initially prescribed to the GCM. Indeed, by doing exactly this, with different GCM's, Niu et al. (2017) produced ice-sheets at LGM ranging from 50 to 150 m SLE and in many cases exceeding the initially prescribed ice-sheet's extent by hundreds of kilometers. We will add a few lines to the manuscript discussing these results in order to clarify this point.

While we agree with the reviewer that the "ultimate" model would require only orbital forcing in order to produce glacial cycles, accurately simulating all the feedbacks between ice-sheets and the atmosphere, the ocean, the carbon cycle and the biosphere, without being in any way "limited" by observations of the past, such a model is beyond the scope of this study.

P14, L6: Added more context to the Conclusions section discussing the results presented by Niu et al. (2017).

Both types of studies share the shortcoming of having no clear
physical cause for the prescribed climatological variations,
 # I would argue that the approach presented herein also has no clear
 # physical cause given the adhoc choice of weights and ignorance of all
 # the other feedbacks from ice sheets to climate..

Although we do not claim that our model captures all existing feedback processes between the climate and the cryosphere, we do believe our model contains several important processes that are not represented in the "glacial index"-type models described in the statement. In these models, a temperature or climate forcing is prescribed based on an external forcing record, regardless of how the ice-sheets inside the model evolve. In our approach, we decouple the contributions to climate change caused by changes in pCO2 and changes in ice-sheet size plus insolation, calculating the latter based on the internal model state through the matrix method. We therefore believe our model set-up to be, though still not as comprehensive as a fully coupled GCM-ISM, at least more physically realistic than the glacial index model described in the statement, especially in the way spatial patterns of climate change are treated.

We will clarify the advantages of our approach in the manuscript.

We will address the reviewer's concerns regarding the "ad hoc choice of weights" later on, when he specifies exactly which choices of weights he finds to be insufficiently motivated.

P3, L9: Added a short paragraph clarifying the difference between the glacial index approach and the matrix method.

Others used dynamically coupled ice-sheet models to Earth System Models..
 # Since you've started a list of alternatives, you should make it complete.
 # IE Should also consider asynchronous and accelerated coupling with GCMS, eg
 # Gregory et al, 2012, and Herrington and Poulsen, 2012.
 # on this same note, should also mention the option of using results from a
 # range of climate models, Eg Tarasov and Peltier, QSR 2004.

We agree that these are valuable references. We will include them in the manuscript.
P2, L17: Added a reference to Tarasov & Peltier (2004) to the list of studies using a glacial-index method to force an ice-sheet model with output from different steady-state GCM simulations.
P2, L25: Added a few lines discussing the work by Herrington & Poulsen and Gregory et al.
P18-22: Added these studies to the list of references.

Difficulties in bridging the differences in model resolution, as well
as other inconsistencies between model states, are addressed and
solved
 # This is a vague arguable claim. Be more precise and accurate as to
 # what you do and do not "solve".

We agree that this statement should be more precise. We will change this in the manuscript.
P3, L20: changed this line to more accurately describe which differences in GCM state and ice-sheet model state need to be accounted for.

the model, we simulate ice-sheets at LGM that agree very well with
geomorphology- based reconstructions
 # This is not true for North America.

We agree that the phrase “very well” might be too optimistic for our simulation of North America. We will change this in the manuscript.

P3, L25: differentiated between Eurasia and North America in our assessment of model performance.

This ensures the constructed climate history is in agreement with the observed 15 pCO2 record and the modelled ice-sheet configuration, thereby capturing the major feedback process between global climate and the cryosphere, where any change in ice-sheet configuration has an immediate impact on local climate through changes in albedo and orographic forcing of precipitation

 # This statement is not justified, especially with the use of only two
 # GCM climate snapshots. Atmospheric circulation and therefore climate
 # will depend non-locally on ice sheet geometry, a dependence that is not captured
 # by two or even a handful of GCM snapshots.

--

P2-L14

Still I'm not convinced how "This ensures the constructed climate history is in agreement with the observed pCO2 record and the modelled ice-sheet configuration". All the climate states other than PI and LGM are interpolations based on some weights, so why should they be in agreement with the actual climatic history? For instance if the jet-stream pattern variation would be a function of a threshold in ice altitude, how would that be captured by interpolation?

We did not intend to claim that the climate history constructed using our two-state climate matrix is a perfect representation of reality. The statement intends to illustrate how the changes in climate simulated by our model are all attributed directly to physical causes (changes in CO_2, ice geometry and insolation) This is in contrast to the inverse forward models discussed earlier in the paragraph, which prescribe changes in temperature based on observations regardless of a clear physical cause. Neither do we claim that either method is better than the other; in the Conclusions section of the manuscript (p12-13) we discuss how the mismatch between data on sea-level and benthic oxygen isotopes on the one hand, both showing a rapid increase in ice volume during the early phase of the glacial cycle, and CO2 and temperature records on the other hand, both indicating a much less rapid cooling, is not solved by either type of model.

We agree that the statement might be interpreted as evidence of overconfidence in our methodology. We will correct this in the manuscript. We will also elaborate further on the various shortcomings and (over)simplifications of our method in the discussion section.

P3, L31: Replaced the discussed statement with a new one that more accurately describes the differences between the inverse modelling approach and ours.

P14, L27: Expanded the discussion of the various shortcomings of our climate parametrization (also in light of the concerns raised by the other reviewer)

It combines the shallow ice approximation (SIA) for grounded ice with the shallow shelf
approximation (SSA) for floating ice shelves to solve the mechanical
 # how are fluxes at the grounding-line handled?
 # How are sub-shelf melt and ice calving treated in this model?

In the transition zone near the grounding line, SIA and SSA ice velocities are combined using the approach by Winkelmann (2011), as explained by de Boer et al. (2013). Sub-shelf melt is calculated based on a combination of the temperature-based formulation by Martin et al. (2011) and the glacial-interglacial parameterization by Pollard & deConto (2009), tuned by de Boer et al. (2013) to produce realistic present-day Antarctic shelves and grounding lines. A more detailed explanation is provided by de Boer et al. (2013) and references therein. Ice calving is treated by simple threshold thickness of 200 m, where any shelf ice below this thickness is removed. We will add more information to the manuscript to clarify this.

P5, L7: Added a few lines detailing the way grounding line fluxes, sub-shelf melt and calving are treated in the model.

Horizontal resolution is 20 km for Greenland and 40 km for the other three regions
 # For future work, I would recommend 20 km or finer grid resolution for non-ensemble best
 # runs

We thank the reviewer for this recommendation.

fig 4:
 # please include present-day continental outlines even under ice using a different
 # colour than the black/grey contours for ice to aid geolocation

We will add these outlines to the figure.

Fig. 1, 4, 7: Added blue lines showing present-day shorelines to the relevant figures.

strongly parameterized -> highly parameterized

We will correct this in the manuscript.
P5, L25: Change "strongly" to "highly".

should reference earlier work, eg EBM climate model coupling to ISMs

We will add more relevant references to the introduction section of the manuscript.
P2, L19: Added references to work by Stap et al. with their EBM-ISM set-up.

eq 1, linear co2 weighting factor
 # given the near logarithmic depending of radiative forcing on pCO2,
 # justify why a linear dependence is imposed

Several preliminary experiments, which we chose not to include in the manuscript, were dedicated to trying out various ways to translate changes in CO2, ice sheet geometry, surface albedo and other model variables into the weighting factors for the climate matrix. We ran experiments with both a linear and a logarithmic dependence of the weighting factor wCO2 on pCO2 and concluded that the difference in outcome was negligible. We will add a line to the manuscript to describe these preliminary experiments and their influence on our choice of parameters.
P6, L9: Added a line to describe these preliminary experiments.

 # eq 5: justify the equal weight contribution for Wco2 and Wice. Given
 # the large variation in insolation changes from the South to North of
 # eg the North American ice sheet complex over a glacial cycle, I
 # don't see how this constant weight mix makes sense.

We feel the reviewer might have misunderstood the way Wice is calculated in the model. This spatially variable weighting factor is calculated based on "absorbed insolation", the product of (1-albedo) and insolation. This links the changes in climate to the two components of this process: changes in insolation (an external forcing) and changes in albedo caused by advancing or retreating ice (a modelled variable) and thereby ensures that the large variations in absorbed insolation caused by the changes in the geometry of the ice-sheet complex are reflected in the calculations.

As with the previous comment, some preliminary experiments, which we chose not to include in the manuscript, were dedicated to finding proper values for the contributions of the two weighting factors. We clarified this in the text.

Sensitivity to the distribution was found to be relatively low; as can be seen from the results in the paper, the temporal evolution of ice volume and CO2 are very similar. This means the values of the two separate weighting factors are usually very close to each other, implying that assigning more weight to one or the other doesn't change the outcome much. Of course, when more weight is given to Wice, at some point the drop in CO2 during the inception doesn't decrease temperatures enough to trigger the inception any more.

We will add a few lines to the manuscript to clarify this.

P7, L9: Added more context to justify this choice of weights.

Gaussian smoothing filter F with
a radius of 200 km, and
 # Why 200 km?

This value is based on earlier work with ANICE by de Boer et al., who used a similar smoothing algorithm to calculate changes in precipitation over the ice-sheet. As before, preliminary experiments not described in the manuscript investigated this parameter and found that results were not very sensitive to its value, so we chose not to change it. We will add a line to the manuscript to clarify this.

P7, L1: Added a few lines to justify the choice of a 200 km smoothing radius.

Since the relative changes in ice-sheet size for Greenland and
Antarctica are much smaller than those for North America and Eurasia,
the changes in absorbed insolation in those regions should have less
impact on local climate. This is reflected in the model by giving more
weight to the pCO2 parameter
 # So why not use this same weighting for the part of Canada covered
 # by the same latitudinal range as Greenland, especially given the
 # proximity of NorthWestern Laurentide/Innuitian ice sheets to Greenland?
 # Why not rely on the 200 km Gaussian radius to take care of the ice sheet
 # scale? I highly suspect that the need for this adhoc change is weighting
 # is due to the lack of accounting for larger scale (eg atmospheric dynamical)
 # effects of ice sheet on climate.

The weighting factor Wice scales the absorbed insolation between two extremes: its maximum value at present-day and its minimum value at LGM. An LGM-sized ice-sheet will therefore always yield a weighting factor of 1 (meaning the GCM LGM simulation is used as forcing), regardless of the absolute change in absorbed insolation. For North America and Eurasia, where the continent changes from virtually ice-free to covered by vast ice-sheets, these changes are very large (a relative change of about 32 % in absorbed insolation integrated over the region). However, for Antarctica and Greenland, the absolute changes in albedo are much smaller, since those regions are already covered by ice at present-day. Even for Antarctica, where the modelled ice volume increases by almost 15 m SLE in our simulation, the change in absorbed insolation integrated over the model region amounts to only 5 %, because the changes in ice area (including shelves) are limited. The effect of changes in Antarctica on regional climate are therefore expected to be smaller than the changes induced by the ice sheets in the Northern Hemisphere. This is reflected in the model by changing the division of the contributions from Wice and Wco2. As before, preliminary experiments not described in the manuscript investigated this distribution and found that results were not much affected.

While we agree that a more elaborate approach, especially taking into account changes in North American ice sheet size into the calculations of Wice for Greenland and Eurasia, along the lines of Abe-Ouchi et al. (2013), would be more realistic, we chose to limit this first model set-up to only first-order effects.

We will add a few lines to the manuscript to clarify this.

P7, L25: Added a few lines to justify the altered wice-wCO2 distribution for Greenland and Antarctica.

eq 10

 # Novel lapse rate approach that addresses a common problem especially

 # for those modellers who rely on a constant lapse rate value.

We fully agree with the reviewer.

eq 10

 # Need to show equation for T(x,y,t) given T_{ref,GCM(x,y)} and lapse_LGM(x,y)

 # As I understand, eq A1 is for de Boer et al 2014, not this paper

 # (since a constant lapse rate is used)

We will add an equation to demonstrate how the new variable lapse-rate is used to calculate surface temperature.

P9, L1: added this extra equation.

P9, L3: fixed several typing errors.

For Greenland and Antarctica, where the changes in ice cover are

relatively small even during glacial cycles, the constant lapse-rate is still applied.
 # justify 8K/km choice

P8-L12
Did you do the same calculation for lapse-rate over Greenland and Antarctica to check how small the difference would be?

We did not do the same calculation for Greenland and Antarctica. We only applied the variable lapse-rate to North America and Eurasia to solve an observed problem, i.e. mean annual surface temperatures increasing instead of decreasing towards LGM over ice-free areas, thus inhibiting ice growth. For Greenland and Antarctica such problems were never observed, so we never applied this method there. The choice of 8 K/km is based on earlier work with ANICE by de Boer et al. (2014) and with the regional climate model RACMO by Helsen et al. (2013). We will add a few lines to the manuscript to clarify this.
P9, L18: added references to de Boer et al. (2014) and Helsen et al. (2013) to justify the 8 K/km choice.

and that the drop in precipitation caused by the ice-plateau-desert effect scales appropriately with ice-sheet size and that the drop in precipitation caused by the ice-plateau-desert effect scales appropriately with ice-sheet size
 # what does "scales appropriately" mean? By what criteria?

This statement only attempts to give a qualitative description. Preliminary experiments not described in the manuscript showed that if only the local ice thickness is used to calculate the weighting factor, precipitation decreases too fast over the main dome, because ice thickness reaches its peak value long before ice extent does. The resulting decrease in mass balance results in modelled ice-sheets that are far too small. By adding ice volume into the weighting factor calculation, precipitation decreases less quickly when the ice grows, allowing the ice-sheet to grow faster and reach its LGM size.
We agree that this is not clear in the manuscript right now. We will add a few lines to the manuscript to clarify this.
P10, L9: Added a few lines explaining the rationale behind including total ice volume in the calculation of the weighting factor.

Similarly, for North America and Eurasia, precipitation is adjusted using the Roe and Lindzen parameterization for wind orography- based correction of precipitation as described in Eq. A3 - A6, but now by using the GCM-generated precipitation and orography as reference

fields instead of their ERA-40 equivalents
 # Why are no orography effects imposed on Greenland? Observed PD
 # fields show such effects

The Roe and Lindzen parameterization described in the manuscript is included in the model to account for changes in orography. For North America and Eurasia this is important, because the flanks of the ice-sheet, where orographic forcing of precipitation occurs, move around over the continent as the ice sheets expand and retreat. For Greenland, the orographic changes are important for present-day but the changes throughout the glacial cycle are much smaller, as the ice flanks hardly migrates. The orographic forcing is already captured in the two GCM snapshots and it is therefore sufficient to use the interpolated states without requiring this correction. We will add a few lines to the manuscript to clarify this.

P10, L20-29: Clarified the explanation of the precipitation calculations and fixed Equation reference numbers.

Although the main dome of the ice-sheets is not
as thick as in the ICE-5G reconstruction
 # this is a good thing

We agree with the reviewer.

Although the main dome of the ice-sheets is not
as thick as in the ICE-5G reconstruction, it now lies more westward than in the
simulation with the 5 default ANICE model,
which is in better agreement with the reconstruction
 # Not clear where you main dome is given the 1000 m contour interval

We agree that this is not clear from the figure. We will add a few extra contour lines to clarify this.

Fig. 1, 4, 7: added an extra contour line at 3500m ice thickness to the relevant figures.

The Antarctic ice-sheet now shows a much stronger increase in ice
volume around LGM, matching the 16 m of eustatic sea-level
contribution postulated by ICE-5G (Peltier, 2004)
 # Should reference more recent literature. The ICE-5G Antarctic
 # ice sheet has little constraint.

However, since it was the ICE- 5G reconstruction that was used as input for the HadCM3 simulation by Singarayer and Valdes (2004), we aim to maintain 30 consistency and reproduce that particular ice-sheet with our model rather than the DATED-1 LGM ice sheet.

 # By what logic? You are assuming that ICE5-G is in conformity with
 # the GCM climate generated using ICE5-G boundary conditions. That is
 # a big assumption. The ice mask leaves a strong climate footprint and
 # so I would expect it not hard to match ICE5-G extent but matching I
 # see no rational to otherwise match ICE5-G topography

While we agree with the reviewer that ICE-5G is hardly perfect and that there is more recent data available for both volume and extent, we believe that a chain of model simulations such as the one performed here (ice-sheet -> GCM -> climate -> ice-sheet model -> ice-sheet) should aim for consistency first, i.e. the ice-sheet produced by the ice-sheet model should match the one that was prescribed to the GCM. Otherwise we'd be prescribing to the ice-sheet model a climate which was calculated based on a different ice-sheet, making it even harder to determine the cause of any observed model-data mismatches.

 # fig 4 and 7
 # add the ICE5-G ice margin extent as say a red
 # contour to these plots to aid comparison
 # also use 500 m ice thickness contours to show more detail (1 km is awfully coarse)

We agree that the requested elements would be of added value, and will add them to the figures.
Fig. 4, 7: Added the ice-5g ice margin and a 3500 m ice thickness contour line.

The southern margin lies a little too far to the north
 # This is an understatement. Be precise

We agree that this statement is imprecise and overly optimistic. We will correct this in the manuscript.
P11, L18: Clarified how far the modelled ice margin and ICE-5G margin lie apart.

Fig 10
 # Please replace this with a sensitivity parameter range that captures

 # say 90% confidence intervals for your parameters. Just switching
 # between PMIP III results from 2 different GCMs will from my
 # experience give a much larger spread in ice sheet volume

We will adapt the figure to make estimating the uncertainty in modelled sea-level arising from the uncertainty in our model parameters more intuitive.

Fig. 10: Replaced lines of individual simulations with ± 2-sigma interval.

regarding Greenland surface temperature anomalies when neglecting the
strong negative excursions during Dansgaard-Oeschger events, which are
not present in our model forcing or 10 climate reference runs and are
also not included as feedback mechanisms in our model physics
 # larger diffs than just missing D/O events in fg 12. Plot 4kyr
 # running mean and you'll see significant diffs.

Modelled temperature anomalies over Greenland and
Antarctica agree well with ice-core isotope-based reconstructions. When
 # not for NGRIP

We agree that the current way the icecore data was plotted made interpreting model-data differences difficult. After subjecting the Greenland records to a 4 ky running mean, we find that modelled surface temperature anomalies fall within the high end of the +- 1 sigma range most of the time.

Fig. 12: Merged the GISP2 and NGRIP records into a single stack. Subjected both the EPICA and Greenland stack records to a 4 ky running mean filter and added 4 ky window standard deviation range.

P13, L18-21: changed the manuscript text to reflect the changes in the figure.

Local monthly ablation Abl is parameterised as a function of the 2-m
air temperature Tano, albedo a and incoming solar radiation at the top
of the atmosphere QTOA, following the approach by Bintanja et
al. (2002):
...
with c1 = 0.0788, c2 = 0.004 and c3 a tuning parameter different for each
individual ice-sheet.
 # equations are dimensionally inconsistent and need dimensional coefficients.

The reviewer is correct, there was a typo in the units of coefficient α. We will correct this, and modify Equations A3 to A6 to be more in line with the original publication by Roe et al. (the current version in the manuscript describes the rather compliated analytical solution of a much more elegant integral).

P15-17: Rewrote the equations described the Roe precipitation in their original, unintegrated form and expanded the explaining text.

These climate states span a two-dimensional climate matrix, with
 # This is not what most modellers would take as a climate matrix

While we agree that a climate matrix consisting of only two GCM snapshots is indeed rather small, we believe our method of model forcing has more in common with the matrix method than the glacial index method – especially because all the algorithms presented in the Methodology section are readily applicable to matrices consisting of more snapshots.
However, we agree with the reviewer that stating that two points span a two-dimensional space is mathematically incorrect. We will correct this in the manuscript.

P6, L1: Changed the relevant sentence to more accurately describe the climate matrix.

calculated temperature between the LGM and PI fields over the ice-free area in the region at LGM.
 # specify region

The region alluded to in this statement is the geographic area covered by the model grid. We will clarify this in the manuscript.

P9, L5: Changed the relevant sentence to clarify which region is meant.

When accounting for uncertainty in the applied forcing and model parameters, the simulated volume of the four major continental ice-sheets (excluding contributions from smaller ice caps, glaciers, thermal expansion and ocean area changes) at LGM amounted to 97 ± 6 m sea-level equivalent.
 # This shows that uncertainties are not adequately addressed. The uncertainties
 # in this modelled system (ie compared to "reality") are going to be much larger than 6 m SLE.

We did not intend to claim that the uncertainties in the applied CO2 forcing and in our ice-sheet model parameters are the only sources of uncertainty in our sea-level reconstruction – merely that those are the only uncertainties that can be meaningfully investigated with this model set-up. We will clarify this difference in the manuscript.

P14, L16: Clarified whence the uncertainty in the quoted number arises.

 # At least 3 of the references to equations in the text have the wrong
 # equation number.

We thank the reviewer for his attention to detail. We will correct the erroneous references.

Entire manuscript: correct all erroneous equation and figure references.

P4-L21
What does "some external forcing" mean?

The full statement, "Surface temperature is calculated from present-day monthly values, including a global temperature offset calculated based on some external forcing, and a constant lapse-rate orographic correction", refers to the way ANICE was used by de Boer et al., Bintanja & van de Wal. In these studies, ANICE was forced using the inverse coupling method, where a global temperature offset is calculated from a benthic oxygen isotope record, icecore isotope record or sea-level record. We agree that this is not clear. Since we do not use this method of forcing and do not allude to it any further, we will remove this statement from the manuscript.

P5, L12: removed this statement.

P4-L28
What is the "existing independent literature"?

de Boer et al. (2013) compared their results to other modelling studies (Huybrechts 2002, Pollard & deConto 2009, Bintanja et al. 2005, Bintanja & van de Wal 2008), geomorphological evidence (Ehlers & Gibbard 2007), sea-level records (Rohling et al 2009, Thompson & Goldstein 2006) and the contribution of ice-sheets to sea-water heavy isotope enrichment (Duplessy et al 2002, Lhomme & Clarke 2005). We will add more references to the manuscript to support our confidence in the ice-sheet model.

P5, L18-22: included the references listed above in the manuscript.

P8-Eq. 11
Why don't you use local altitude instead of the ice-thickness? The

difference at LGM could reach 1 km and it is surface elevation that physically matters.

Since the ice thickness is scaled between two extremes (LGM value and zero) to calculate the weighting factor (which scales between 0 and 1), using surface elevation instead of ice thickness will yield the same result as long as the two variables change at the same rate. During the build-up phase of the glacial cycle this is generally true (the ice rarely grows faster than the lithosphere can adjust). During the deglaciation it is not, but since that process is dominated by ablation rather than accumulation, we believe changing the parameterization from ice thickness to surface elevation will not significantly impact our results.

P8-L16

"Whereas a continental-sized ice-sheet influences temperature mainly through albedo"; is this true? What about changes in atmospheric circulation, runoff and therefore changes in ocean circulation, and the elevation itself, hence the lapse-rate effect?

We agree that this statement is incorrect – the changes in temperature are caused not only by changes in albedo but indeed also other processes, not all of which are captured by our model set-up. We will change this in the manuscript.

P9, L20-23: Changed the statement so that it only illustrates why the choice was made to use a different parametrization for precipitation than the one for temperature without seeming to suggest that the current temperature parameterization captures all possible processes.

Fig. 6

The total ice volume evolution, specially during the inception phase, doesn't follow the records; eg the 110 ka max volume.

The mismatch between our own modelled ice volume evolution and available records during the early part of the glacial cycle is discussed in the Conclusions section of the manuscript (page 12 – 13). We will add the ICE-5G pre-LGM eustatic sea-level record to Figure 6 to illustrate this mismatch.

Fig. 6: Added the ICE-5G pre-LGM eustatic sea-level contribution record to the figure.

Application of HadCM3@Bristolv1.0 paleo simulations as forcing for an ice-sheet model, ANICE2.1: set-up and benchmark experiments

Constantijn J. Berends[1], Bas de Boer[1], Roderik S. W. van de Wal[1]

[1]Institute for Marine and Atmospheric research Utrecht, Utrecht University, The Netherlands

Correspondence to: Constantijn J. Berends (c.j.berends@uu.nl)

Abstract. Fully coupled ice-sheet-climate modelling over 10,000 – 100,000-year time scales on high spatial and temporal resolution remains beyond the capability of current computational systems. Hybrid GCM-ice-sheet modelling offers a middle ground, balancing the need to accurately capture both long-term processes, in particular circulation driven changes in precipitation, and processes requiring a high spatial resolution like ablation. Here, we present and evaluate a model set-up that forces the ANICE 3D thermodynamic ice-sheet-shelf model calculating the four large continental ice-sheets (Antarctica, Greenland, North America and Eurasia), with pre-calculated output from two steady-state simulations with the HadCM3 general circulation model (GCM), using a so-called matrix method of coupling both components, where simulations with various levels of pCO_2 and ice-sheet configuration are combined to form a time-continuous transient climate forcing consistent with the modelled ice-sheets. We address the difficulties in downscaling low-resolution GCM output to the higher-resolution grid of an ice-sheet model, and account for differences between GCM and ice-sheet model surface topography ranging from interglacial to glacial conditions. Although the approach presented here can be applied to a matrix with any number of GCM snapshots, we limited our experiments to a matrix of only two snapshots. As a benchmark experiment to assess the validity of this model set-up, we perform a simulation of the entire last glacial cycle, from 120 kyr ago to present-day. The simulated eustatic sea-level drop at the Last Glacial maximum (LGM) for the combined Antarctic, Greenland, Eurasian and North-American ice-sheets amounts to 100 m, in line with many other studies. The simulated ice-sheets at LGM agree well with the ICE-5G reconstruction and the more recent DATED-1 reconstruction in terms of total volume and geographical location of the ice sheets. Moreover, modelled benthic oxygen isotope abundance and the relative contributions from global ice volume and deep-water temperature agree well with available data, as do surface temperature histories for the Greenland and Antarctic ice-sheets. This model strategy can be used to create time-continuous ice-sheet distribution and sea-level reconstructions for geological periods up to several millions of years in duration, capturing climate model driven variations in the mass balance of the ice sheet.

1 Introduction

Sea-level rise due to large-scale retreat of the Greenland and Antarctic ice-sheets poses one of the main long-term risks of climate change (Church et al., 2013). However, accurate projections of the magnitude and rate of retreat are limited by our understanding of the feedback processes between global climate and the cryosphere on centennial to multi-millennial time-

Deleted: A hybrid GCM paleo ice-sheet model, ANICE2.1 – HadCM3@Bristolv1.0: set up and benchmark experiments

Deleted: all ice on Earth

Deleted: several

scales. One way to test the performance of ice-sheet models that are used for these future projections, is to apply these models to ice-sheet evolution in the geological past, both during glacial periods with more ice than present-day, and warmer periods with less ice (e.g. Bamber et al., 2009; Pollard and DeConto, 2009; de Boer et al., 2013; Dutton et al., 2015).

Ideally, such a model set-up would consist of a general circulation model (GCM) fully coupled to an ice-sheet model, exchanging information every model time-step. However, whereas the computational load of typical ice-sheet models allows simulations of 10,000 – 100,000 years to be carried out within a reasonable amount of time, climate models are much more computationally demanding, limiting simulation time to decadal or centennial time-scales. Fully coupled ice-sheet-climate modelling of complete glacial cycles is therefore not feasible with the current state of model infrastructure.

In order to gain insight in the long-term interactions between the climate and the cryosphere despite these computational limitations, different solutions have been proposed in the past. Several studies of past glacial cycles using ice-sheet models (Bintanja et al., 2002; de Boer et al., 2014) apply a present-day climate with a uniform temperature offset based on a "glacial index", usually from ice-core isotope records, adapting precipitation based on a Clausius-Clapeyron type relationship. Others have used a similar glacial index to create a linear combination of output of different GCM time-slice simulations (Marshall et al., 2000, 2002; Charbit et al., 2002, 2007; Tarasov and Peltier, 2004; Zweck and Huybrechts, 2005; Niu et al., 2017). Both types of studies share the shortcoming of having no clear physical cause for the prescribed climatological variations, and no explicit feedback from the cryosphere back onto the prescribed climate. Stap et al. (2014; 2016) used a zonally averaged energy balance model coupled to a one-dimensional ice-sheet model to simulate the behaviour of global climate and the cryosphere over millions of years, trading regional details for the ability to simulate long-term feedback processes. Others used dynamically coupled ice-sheet models to Earth System Models of Intermediate Complexity (Charbit et al., 2005; Ganopolski et al., 2010). This approach comes closer to the ideal case of an ice-sheet model fully coupled to a GCM, but since EMICs typically have a coarse spatial resolution, processes influencing the surface mass balance variably over the different parts of the ice-sheet (e.g. precipitation, ablation) still need to be parametrised. Other studies have asynchronously coupled ice-sheet models to GCMs (Herrington and Poulsen, 2012), or used fully-coupled ice-sheet-GCM set-ups with low-resolution GCMs for shorter periods of model time (Gregory et al., 2012), all showing that non-linear and non-local processes can significantly affect the behaviour of ice-sheets under a changing climate. Abe-Ouchi et al. (2013) performed a very detailed decoupling of the effects on climate of changes in pCO_2, albedo, surface elevation and atmospheric circulation based on several GCM snapshots and used these to force an ice-sheet model in a manner similar to both the glacial index method and the method described in this manuscript.

The "matrix method" of hybrid ice-sheet-climate modelling (Pollard, 2010; Pollard et al., 2013) is based on a collection of steady-state GCM simulations where different values for one or more parameters such as pCO_2, insolation or global ice coverage are used to construct a so-called "climate matrix". By varying these parameters continuously over time and

interpolating between these pre-calculated climate states, a time-continuous climate history can be constructed, which can be used to force an ice-sheet model. Pollard et al. (2013) used this method to simulate the evolution of the Antarctic ice-sheet during the early Oligocene for 6 million years, using a 40km resolution ice-sheet model forced with output from the GENESIS version 3 GCM. They concluded that the method had some drawbacks, including a crude albedo feedback, and inability to smoothly track orographic precipitation, but that it was adequate for studying the large-scale ice-sheet evolution in which they were interested.

An important difference between the glacial index approach and the matrix method is the latter's more explicit description of the feedback of an expanding or retreating ice-sheet on local, regional and global climate. In a glacial index model, the temporal evolution of the prescribed climatology is determined by an external forcing record (typically pCO_2, benthic $\delta^{18}O$ or ice-core isotopes). The matrix method combines this external forcing with one or more internally modelled parameters (typically ice volume or extent) to determine the applied climatology, thus allowing changes in ice-sheet configuration to feed back on climate.

In this study, we constructed a model set-up with a climate matrix consisting of two simulations with the HadCM3 GCM. The climate that is obtained from this matrix, based on the prescribed atmospheric CO_2 concentration and internally modelled ice-sheets, is applied to the mass balance module of the ANICE ice-sheet model, which simulates the evolution of all four major continental ice-sheets (North America, Eurasia, Greenland and Antarctica) simultaneously. Difficulties in bridging the differences in model resolution and differences in ice-sheet configuration between GCM and ice-sheet model state, especially regarding the orographic forcing of precipitation resulting from ice-sheet advance, are addressed and overcome. As a benchmark experiment, a simulation of the entire last glacial cycle, from 120 kyr to present-day, was performed with this model set-up. We show that, because of several improvements to the way changes in albedo and precipitation are handled by the model, we simulate ice-sheets at the Last Glacial Maximum (LGM) that agree very well with geomorphology-based reconstructions for Eurasia and better than previous ANICE versions for North America.

Deleted: , as well as other inconsistencies between model states, are addressed and solved

Previous work with the ANICE ice-sheet model (de Boer et al., 2013, 2014) used an inverse coupling method, where a global temperature offset is calculated in every model time-step such that the resulting deep-water temperature, combined with simulated global ice volume, matches a prescribed $\delta^{18}O$ record. This approach essentially determines how global climate should have behaved in order to produce the observed $\delta^{18}O$ record - regardless of what, if anything, could have caused the resulting strong, rapid climatic variations. Instead of working back from the a posteriori result of benthic $\delta^{18}O$, the new approach presented here starts with the a priori forcings of insolation and pCO_2 and determines what global climate should have looked like based on the forcings and the modelled ice-sheets. Although this still does not solve the discrepancy between the rapid cooling and sea-level drop suggested by the $\delta^{18}O$ record and sea-level data on the one hand, and the much more

gradual decline in pCO_2 and surface temperature shown in the ice cores on the other that was observed by other studies (Bintanja and van de Wal, 2008; van de Wal et al., 2011; de Boer et al, 2014; Niu et al., 2017) it might provide new insights on the cause of this discrepancy.

Deleted: The new model set-up presented here differs from this approach in that we use the climate matrix to determine what global climate (both temperature and precipitation according to a GCM) would have looked like for a certain prescribed pCO_2 and modelled ice-sheet configuration, where the latter is calculated by the ice-sheet model, which is forced by this prescribed climate state. This ensures the constructed climate history is in agreement with the observed pCO_2 record and the modelled ice-sheet configuration, thereby capturing the major feedback process between global climate and the cryosphere, where any change in ice-sheet configuration has an immediate impact on local climate through changes in albedo and orographic forcing of precipitation, and any change in climate changes the mass balance of the ice-sheet.

2 Methodology

2.1 Climate model

HadCM3 is a coupled atmosphere-ocean general circulation model (Gordon et al., 2000; Valdes et al., 2017). It has been shown to be capable of accurately reproducing the heat budget of the present-day climate (Gordon et al., 2000) and has been used for future climate projections in the IPCC AR4 (Solomon et al., 2007) as well as palaeoclimate reconstructions such as PMIP2 (Braconnot et al., 2007) and PlioMIP (Haywood and Valdes, 2003; Dolan et al., 2011, 2015; Haywood et al., 2013). The atmosphere module of HadCM3 covers the entire globe with grid cells of 2.5 ° latitude by 3.75 ° longitude, giving a north-south resolution of about 278 km, whereas east-west resolution varies from about 70 km over northern Greenland (80 ° latitude) to about 290 km over southern Canada (45 ° latitude, the southern-most area covered by the ANICE grid). The ocean is modelled at a horizontal resolution of 1.25 ° by 1.25 °, with 20 vertical layers.

In their 2010 study, Singarayer and Valdes used HadCM3 to simulate global climate during LGM, pre-industrial (PI) and several time slices in between. Orbital parameters representative of the era are used according to Laskar et al. (2004), atmospheric CO2 concentration is prescribed according to the Vostok ice-core record (190 ppmv at LGM; Petit et al., 1999; Loulergue et al., 2008) and orographic forcing follows the ICE-5G ice distribution reconstruction by Peltier (2004), shown in Fig. 1. Temperature and precipitation fields resulting from these two experiments are shown in Fig. 2 and Fig. 3.

Deleted: the Last Glacial Maximum (

Deleted:)

The modelled glacial-interglacial global mean temperature difference is 4.3 K, which is in good agreement with results from other model studies (Hewitt et al., 2001; Braconnot et al., 2007), as well as reconstructions from multiple proxies (Jansen et al., 2007; Annan and Hargreaves, 2013). Comparisons of the model results with ice core isotope temperature reconstructions from Greenland (GRIP; Masson-Delmotte et al., 2005) and Antarctica (EPICA dome C; Jouzel et al., 2007), as well as borehole-derived surface temperature reconstructions (Dahl-Jensen et al., 1998) indicate that glacial-interglacial temperature changes at these high latitudes are slightly underestimated by the model, by up to 1.5 K over Antarctica and up to 4 K over Greenland.

Deleted: °C

2.2 Ice-sheet model

To simulate the ice evolution on Earth we use ANICE, a coupled 3-D ice-sheet-shelf model (Bintanja and Van de Wal, 2008; de Boer et al., 2013, 2014, 2015). It combines the shallow ice approximation (SIA) for grounded ice with the shallow shelf approximation (SSA) for floating ice shelves to solve the mechanical equations and incorporates a thermodynamical module

to calculate internal ice temperatures. In ANICE, the applied mass balance is calculated using the parameterization by Bintanja and van de Wal (2005, 2008), which uses present-day monthly precipitation values, where changes in precipitation follow from a Clausius-Clapeyron relation as a function of free atmospheric temperature. Time- and latitude-dependent insolation values according to the reconstruction by Laskar et al. (2004) are used to prescribe incoming radiation at the top of the atmosphere. Ablation is calculated using the surface temperature-albedo-insolation parameterization by Bintanja et al. (2002). In the transition zone near the grounding line, SIA and SSA ice velocities are averaged using the approach by Winkelmann (2011), as explained by de Boer et al. (2013). Sub-shelf melt is calculated based on a combination of the temperature-based formulation by Martin et al. (2011) and the glacial-interglacial parameterization by Pollard & DeConto (2009), tuned by de Boer et al. (2013) to produce realistic present-day Antarctic shelves and grounding lines. A more detailed explanation is provided by de Boer et al. (2013) and references therein, including a figure of the model grid. Ice calving is treated by simple threshold thickness of 200 m, where any shelf ice below this thickness is removed. ANICE calculates ice sheet evolution on four separate grids simultaneously, covering the areas of the large Pleistocene ice-sheets: North America, Eurasia, Greenland and Antarctica. Horizontal resolution is 20 km for Greenland and 40 km for the other three regions.

In their 2013 study, de Boer et al. simulated global ice distribution and sea level variation over the last 1 million years, forcing ANICE with the LR04 benthic $\delta^{18}O$ record using an inverse routine. Their simulated LGM ice-sheets are shown in Fig. 4. They showed that their results are in good agreement with existing independent literature in terms of sea-level contributions (Rohling et al., 2009; Thompson and Goldstein, 2006), sea-water heavy isotope enrichment (Duplessy et al., 2002; Lhomme and Clarke, 2005) and other modelling studies (Huybrechts, 2002; Bintanja et al., 2005; Bintanja and van de Wal, 2008; Pollard and DeConto, 2009), although ice-sheet location and extent do not agree well with evidence from geomorphology (Ehlers and Gibbard, 2007; de Boer et al., 2013 and references therein). The latter is likely a result from the absence of feedback from the growth of large ice-sheets onto large-scale atmospheric circulation patterns in the model, e.g. failing to reproduce the decrease in precipitation over the Barents Sea – Kara Sea area caused by the appearance of the large Fennoscandian ice dome, resulting in the appearance of an unrealistically large ice dome over the Barents Sea. The highly parameterized climate forcing and resulting computational efficiency of ANICE allow these transient simulations of multiple glacial cycles to be carried out within 10 – 100h on single-core systems, making ensemble simulations feasible.

2.3 Climate matrix forcing

A climate matrix, as defined by Pollard (2010), is a collection of output data from different steady-state GCM simulations that differ from each other in one or more key parameters or boundary conditions, such as prescribed atmospheric pCO_2, orbital configuration or ice-sheet configuration. At every point in time during the simulation, the location of the model state within this matrix is extracted from the matrix by interpolating between its constituent pre-calculated climate states. The pair of climate states generated by Singarayer and Valdes (2010) using HadCM3 is based on otherwise identical input parameters that differ in two respects: pCO_2 and ice-sheet coverage. These climate states can be viewed as points a two-dimensional climate

Deleted: Surface temperature is calculated from present-day monthly values, including a global temperature offset calculated based on some external forcing, and a constant lapse-rate orographic correction.

Deleted: 4

Deleted: 400 kyr

Deleted: the

Deleted: by de Boer et al. (2013)

Deleted: modelled variations in sea-level, global mean temperature and benthic $\delta^{18}O$

Deleted: strongly

Deleted: span

matrix, with pCO_2 constituting one dimension and ice-sheet coverage constituting another. In order to calculate a climate state for intermediate pCO_2 and ice-sheet coverage values, simple weight functions yielding linear interpolation in this climate phase-space will yield the corresponding monthly temperature and precipitation fields.

The weighting factor w_{CO2} is calculated as:

$$w_{CO2} = \frac{pCO_2 - pCO_{2,LGM}}{pCO_{2,PI} - pCO_{2,LGM}}, \quad (1)$$

with $pCO_{2,PI}$ = 280 ppmv and $pCO_{2,LGM}$ = 190 ppmv. Although the dependence of radiative forcing on pCO_2 is more logarithmic than linear, preliminary experiments showed over this range results are nearly identical. To determine the position of the model state along the pCO_2 dimension of the climate matrix, we use the EPICA ice core record by Lüthi et al. (2008). However, the ice-sheet coverage dimension of the matrix, described by w_{ice}, is more complicated and cannot be adequately described by a single scalar weight function. Since a continental-sized ice-sheet affects both local and global temperature mainly because of the increase in albedo, we chose to represent this process in the model by making the ice-sheet coverage dimension of the climate matrix a spatially variable field $w_{ice}(x, y)$, calculated by scaling between the local absorbed insolation at present-day and at LGM. In this way the albedo feedback is captured more realistically. The absorbed insolation I_{abs} is calculated by multiplying incoming insolation at the top of the atmosphere Q_{TOA} (from Laskar et al., 2004) with the surface albedo α, the latter being calculated internally by ANICE:

$$I_{abs}(x, y) = \big(1 - \alpha(x, y)\big) \cdot Q_{TOA}(x, y). \quad (2)$$

The weighting field is calculated by scaling between the PI and LGM reference fields:

$$w_{ins}(x, y) = \frac{I_{abs,mod}(x, y) - I_{abs,LGM}(x, y)}{I_{abs,PI}(x, y) - I_{abs,LGM}(x, y)}, \quad (3)$$

running from 0 at the LGM to 1 for the PI. To account for both local and regional effects, a Gaussian smoothing filter F with a radius of 200 km, and a total average value are added to the weighting field:

$$w_{ice}(x, y) = \tfrac{1}{7} w_{ins}(x, y) + \tfrac{3}{7} F\big(w_{ins}(x, y)\big) + \tfrac{3}{7} \overline{w_{ins}}, \quad (4)$$

with the weights of the respective unsmoothed, smoothed and average values determined experimentally. The value of 200 km for the smoothing radius is based on de Boer et al. (2014), who used a similar smoothing procedure in their precipitation model.

Preliminary experiments showed that the sensitivity of modelled ice volume to the value of this parameter was quite low. For all four ice-sheets, these spatially variable ice weighting fields are combined with the scalar pCO_2 weight w_{CO2} to yield the final weighting parameter w_{tot}:

$$w_{tot} = \frac{w_{CO2} + w_{ice}}{2}, \quad (5)$$

which is used to linearly interpolate between the states in the climate matrix and calculate the reference temperature, precipitation and orography. Preliminary experiments showed that the sensitivity of the modelled ice volume to the distribution of contributions from w_{CO2} and w_{ice} is quite low. Since the two variables generally show coherent temporal behaviour, the two weighting factors are usually close together, meaning w_{tot} doesn't change much when altering the distribution. When too much weight is given to w_{ice}, eventually a threshold is reached where the drop in pCO_2 during the early phase of the glacial cycle doesn't result in a strong enough cooling to trigger the growth of ice, thus breaking down this similarity.

Precipitation is customarily interpolated logarithmically to accurately reflect relative changes and to prevent the occurrence of negative values:

$$T_{ref,GCM}(x,y) = w_{tot} \cdot T_{PI}(x,y) + (1 - w_{tot}) \cdot T_{LGM}(x,y), \quad (6)$$

$$P_{ref,GCM}(x,y) = e^{\left(w_{tot} \cdot log\left(P_{PI}(x,y)\right) + (1-w_{tot}) \cdot log\left(P_{LGM}(x,y)\right)\right)}, \quad (7)$$

$$h_{ref,GCM}(x,y) = w_{tot} \cdot h_{PI}(x,y) + (1 - w_{tot}) \cdot h_{LGM}(x,y). \quad (8)$$

Being linear combinations of output data from a relatively low-resolution GCM, these three data fields necessarily have a lower resolution than the ice-sheet model to which they will be applied. To correct for this, the temperature and precipitation are adapted based on the difference between the interpolated reference orography $h_{ref,GCM}$ and the actual model orography, using the approach by de Boer et al. (2013) described in Appendix A.

Since the relative changes in ice-sheet size for Greenland and Antarctica are much smaller than those for North America and Eurasia, the relative changes in absorbed insolation in those regions are proportionally smaller and should therefore have had less impact on local climate. For example, for North America the total absorbed insolation over the model grid at LGM is 32 % lower than at present-day, whereas for Antarctica this change is only 5 %. This is reflected in the model by giving more weight to the pCO_2 parameter:

$$GRL, ANT: w_{tot} = \frac{3 \cdot w_{CO2} + w_{ice}(x,y)}{4}. \quad (9)$$

Preliminary experiments showed that here too, the sensitivity of the modelled ice volume to this distribution is relatively low.

2.4 Lapse rate

One of the major simplifications in the ANICE mass balance model is the assumption that temperature decreases linearly with altitude - the spatially and temporally constant lapse-rate of -8 K/km. As has been shown by de Boer et al. (2014), the methodology of combining this constant lapse-rate with a global temperature offset derived from external forcing produced realistic results in terms of global and regional ice volume when simulating Pleistocene glacial cycles. However, even though the reference orography field obtained from the climate matrix is already close to the model orography and the correction applied to the GCM reference temperature field is therefore much smaller, preliminary experiments showed that even making these relatively small corrections using a constant lapse-rate resulted in distorted results.

The limitations of this constant lapse rate procedure can be seen over the western part of Canada, an area that is hypothesized to have remained ice-free for the larger part of the last glacial cycle until a few thousand years before LGM. Here, results from the LGM experiment with HadCM3 (Singarayer and Valdes, 2010) indicate mean annual surface temperatures of around 235 K, or -38 °C. When calculating this surface temperature following the approach by de Boer et al. (2014), starting with the present-day surface temperature at bedrock and scaling with the constant lapse-rate of -8 K/km to the ice-sheet surface (with an ice thickness of up to 5000 m, as indicated by ICE-5G), the resulting value is about 220 K, or -53 °C, about 15 degrees colder than calculated with the GCM, as shown in Fig. 5. A problem occurs during the inception and the subsequent build-up towards LGM, when this area is still ice-free in the model. Using the GCM-generated temperature field as a reference and scaling this down to bedrock level will then result in surface temperatures that are actually warmer than present-day. This is unlikely and results in overestimated melt rates near the ice margins.

A solution to this is to slightly adapt the constant lapse-rate approximation. Assuming the GCM-generated temperature field at LGM is still based upon the present-day temperature field plus a global offset and a (local) lapse-rate correction, similar to the old ANICE method, this local lapse-rate correction field is then calculated as:

$$\lambda_{LGM}(x,y) = -\frac{T_{LGM}(x,y) - (T_{PI}(x,y) + \Delta T_{LGM})}{h_{LGM}(x,y) - h_{PI}(x,y)}, \quad (10)$$

, and the downscaling from the GCM grid to the ice model grid, previously described by Eq. A1, now being calculated as:

$$T(x,y) = T_{ref}(x,y) + \lambda_{LGM}(x,y)\left(h(x,y) - h_{ref}(x,y)\right). \quad (11)$$

where the local lapse-rate at LGM, λ_{LGM}, is calculated by dividing the difference between the local GCM-calculated surface temperature, T_{LGM}, and the extrapolated temperature at local bedrock altitude, $T_{bed}(x,y,t) = T_{PI}(x,y,t) + \Delta T_{LGM}$, by the change in local orography, h_{LGM}, with respect to present-day (h_{PI}). The temperature offset ΔT_{LGM} is the mean difference in GCM-calculated temperature between the LGM and PI fields over the ice-free area in the respective model region (either North America or Eurasia) at LGM. For North America, this results in a value of $\Delta T_{LGM} = -14.9$ K. This methodology ensures that when the modelled ice-sheet is identical to the ICE-5G ice-sheet at LGM and the CO_2 concentration is at the LGM value (190 ppmv pCO_2), the temperature field that is used to calculate the mass balance is still identical to the GCM-calculated temperature field. It also guarantees that, when pCO_2 is at 190 ppmv but no ice is present in the model, mean annual surface temperatures are uniformly lower than present-day by ΔT_{LGM}.

Of course, the latter scenario only occurs during non-physical steady-state experiments such as forcing ANICE with the LGM GCM climate but initializing with present-day ice cover. During transient experiments, the modelled ice-sheets generally resemble those "expected" by the mass balance model through the climate state on which it is based, that the applied lapse-rate correction is generally small. This variable lapse-rate solution is used in the surface mass balance models for North America and Eurasia, since those regions see the dramatic changes in orography that require this correction. For Greenland and Antarctica, where the changes in ice cover are relatively small even during glacial cycles, the constant lapse-rate is still applied with a value of 8 K/km based on earlier work with ANICE by Helsen et al. (2013) and de Boer et al. (2014).

2.5 Precipitation

Present-day observations from Greenland indicate that the effect a continental-sized ice-sheet has on local precipitation is mostly due to geometry; more precipitation falls on the flanks due to orographic forcing, and as a result the dome becomes a plateau desert (Roe and Lindzen, 2001; Roe, 2002). The different character of this process calls for a different representation in the model than the absorbed insolation-based temperature calculation. In order to calculate monthly precipitation values, for North America and Eurasia we use the "local ice-weighting" method described by Pollard (2010). For every element of the spatial grid, ice thickness relative to the ice thicknesses at that element for the different reference GCM states, limited by the total volume of the ice-sheet, is used to obtain the interpolation parameter for the ice dimension of the climate matrix. The interpolation parameter for the "ice" dimension of the climate matrix w_{ice} is expressed as:

$$w_{ice}(x,y) = \frac{Hi_{mod}(x,y) - Hi_{PI}(x,y)}{Hi_{LGM}(x,y) - Hi_{PI}(x,y)} \cdot \frac{V_{mod} - V_{PI}}{V_{LGM} - V_{PI}}, \quad (12)$$

Deleted: temperature

Deleted: s

Deleted: the forcing parameters is at the LGM values,

Deleted: .

Deleted: Whereas a continental-sized ice-sheet influences temperature mainly through albedo, t

Deleted: 1

where Hi_{mod} is the modelled local ice thickness and Hi_{PI} and Hi_{LGM} are the local ice thickness values in the reference fields from the GCM states. V_{mod}, V_{PI} and V_{LGM} are the modelled and reference ice-sheet volumes. For Greenland and Antarctica, only the total ice volume limitation is applied and the interpolation weight is calculated as:

$$w_{ice}(x,y) = \frac{V_{mod} - V_{PI}}{V_{LGM} - V_{PI}}. \quad (13)$$

The first term in Eq. 12 describes the local ice weighting method by Pollard (2010), whereas the second term describes the total ice volume scaling. Combining these two terms ensures that precipitation prescribed to the model only decreases over areas where the model actually simulates ice, and that the drop in precipitation caused by the ice-plateau-desert effect scales appropriately with ice-sheet size. Since the thickness of a growing ice-sheet levels off much earlier than its horizontal extent, an ice-sheet of only a quarter of its LGM extent can already have nearly the same maximum thickness. Scaling precipitation based on local thickness alone will therefore result in the ice plateau becoming too dry too early in the growth phase, limiting further growth. Preliminary experiments showed that including the total ice-sheet volume in the calculation of the weighting factor solved this problem, resulting in a growth rate more in line with expectations from sea-level records.

The reason that the local ice thickness term is absent in the calculation for Greenland and Antarctica shown in Eq. 13 is that the ICE-5G LGM ice-sheets that were used to calculate the corresponding GCM states are, in many places, thinner at LGM than at present-day, even though the total volume of the ice-sheet is larger. This would mean that an increase of modelled ice thickness would lead to an increase in applied local precipitation, causing unrealistic ice growth. Therefore, in order to prevent such unrealistic scenarios, precipitation is scaled only by the total ice-sheet volume.

For Greenland and Antarctica, the reference GCM precipitation field $P_{GCM,ref}$, is downscaled from the GCM to the ice-sheet model resolution based on the difference in temperature between the model state T_{mod} and the reference GCM state T_{GCM}, as shown in Eq. 14, according to a Clausius-Clapeyron relationship, similar to the approach by de Boer et al. (2014) described in Appendix A. This ensures that smaller scale topographical features present in the model but not in the lower resolution GCM have an influence on local precipitation through their effect on local surface temperature.

$$P_{mod}(x,y) = P_{GCM,ref}(x,y) \cdot 1.0266^{(T_{mod}(x,y) - T_{GCM}(x,y))} \quad (14)$$

Similarly, for North America and Eurasia, precipitation is adjusted using the Roe (2002) parameterization for wind-orography-based correction of precipitation as described in Eq. A3 - A6, but now by using the GCM-generated precipitation and orography as reference fields instead of their ERA-40 equivalents. This allows for a better representation of orographic forcing of precipitation on the migrating ice flanks as these ice-sheets advance and retreat, an effect that cannot be captured by interpolating by different GCM snapshots alone.

Deleted: 2
Deleted: 0
Deleted: 1
Deleted: adjusted
Deleted: to account for
Deleted: 2
Deleted: 3

3 Results

3.1 Last glacial cycle benchmark

As a benchmark experiment, the new model set-up was used to perform a simulation of the last glacial cycle. The climate matrix for this experiment consists solely of the PI_Control and LGM experiments by Singarayer and Valdes (2010). Following the approach by Bintanja et al. (2002), the model was tuned by adjusting the ablation parameter c_3 in Eq. A9 individually for all four ice-sheet regions, such that their modelled sea-level contribution at LGM matched the values postulated by ICE-5G (Peltier, 2004). The resulting c_3 values, which are hereafter kept fixed, are shown in Table 1. This 120 kyr simulation took about 12 hours to complete on a single-processor system, meaning it is feasible to use this model set-up to perform ensemble simulations without demanding excessive amounts of computation time.

Shown in Fig. 6 are the results of this experiment in terms of the global mean sea-level contributions of the four separate ice-sheets over time, as well as the total global mean sea-level, together with the same values from a simulation of the same period of time with the default ANICE model forced with the LR04 benthic $\delta^{18}O$ record using an inverse routine. As can be seen, the new model set-up obtains a close match to the postulated ICE-5G LGM ice volume for all ice-sheets except Greenland. The resulting ice-sheets at LGM are shown in Fig. 7. As can be seen, the north-west Canadian corridor is now blocked by ice, which was still open in the default ANICE simulation shown earlier in Fig. 4. Although the main dome of the ice-sheets is not as thick as in the ICE-5G reconstruction, it now lies more westward than in the simulation with the default ANICE model, forming a ridge running from mid-west Canada to the eastern shores of Hudson Bay, which is in better agreement with the reconstruction. The southern margin lies too far to the north, varying from 400 km near the Atlantic coast to up to 950 km in the mid-west. The Antarctic ice-sheet now shows a much stronger increase in ice volume around LGM, matching the 16 m of eustatic sea-level contribution postulated by ICE-5G (Peltier, 2004). Most of the growth ice mass increase takes place happens in West Antarctica - as can be seen, both the Ross and Ronne shelves become fully grounded. The Greenland ice-sheet does show some minor growth over the glacial cycle, though not as much as postulated. It must be noted that several modelling studies of Greenland using the ANICE model (de Boer et al., 2013, 2014) have had trouble in this regard, mostly because of the difficulty in simulating the ice-shelves that might have formed around the continent at the time but are not there now (Bradley et al., 2018).

The simulated Eurasian ice-sheet is now in better agreement with the consensus regarding the Fennoscandian dome, as well as with the total ice volume or sea-level contribution. When simulated with the default ANICE version, the main dome of the Eurasian ice-sheet forms over the Barents Sea, extending eastward to about 70°E. The new model set-up results in a dome over Fennoscandia and a smaller dome over the Barents Sea. The present-day southern North Sea area, formerly Doggerland, remains ice-free, in agreement with paleo data (Hughes et al., 2016). Compared to the recent DATED-1 reconstruction of the Eurasian ice-sheet (Hughes et al., 2016) at LGM shown in Fig. 8, the modelled ice-sheet does not extend as far south over

Deleted: a little

Deleted: especially

northern Germany, Poland and Lithuania. The simulated Atlantic side of the ice margin agrees well with the reconstruction, reaching the edge of the continental shelf everywhere.

Peltier (2004) provides an ice volume of the Eurasian ice-sheet of about 17 m sea-level equivalent based on GPS observations of isostatic rebound, whereas Hughes et al. (2016) state a volume of 24 m based on geomorphological evidence of the extent and a logarithmic linear regression between ice sheet area and volume. By slightly increasing the ablation tuning parameter, thus decreasing ablation and increasing ice volume, we were able to produce a Eurasian ice-sheet with a volume of 24 m sea-level equivalent that matches the DATED-1 horizontal extent very well, as shown in Fig. 9. However, since it was the ICE-5G reconstruction that was used as input for the HadCM3 simulation by Singarayer and Valdes (2004), we aim to maintain consistency and reproduce that particular ice-sheet with our model rather than the DATED-1 LGM ice sheet. We will therefore not use this new version as our benchmark.

3.2 Sensitivity to forcing and model parameters

In order to estimate the uncertainty in modelled global mean sea-level following from the uncertainty in the EPICA pCO_2 record, we performed simulations with the forcing record adjusted to its respective upper and lower bounds, based on an LGM uncertainty of 10 ppmv (Lüthi et al., 2008). Additionally, we investigated the model sensitivity to the four ablation tuning parameters c_3 for the different ice-sheets mentioned earlier by performing simulations where these parameters had been either increased or decreased by 10% relative to their benchmark value. We also assessed model sensitivity to the SSA and SIA flow enhancement factors, with the upper and lower limits determined by Ma et al. (2010) in order to test the sensitivity to the ice sheet dynamics. Results from these different sensitivity tests are shown in Fig. 10. The resulting uncertainty in simulated LGM ice volume amounts to about 6 m sea-level equivalent in either direction, about 6 % of the total signal, for both the CO_2 and ablation parameter experiments. Sensitivity to the flow enhancement factor ratio is lower at about 4 % of the total signal.

3.3 Benthic oxygen isotope abundance

Included in ANICE is a module that tracks the oxygen isotope abundances of the ocean ($\delta^{18}O_{sw}$), precipitation and the ice-sheets. In the default ANICE version, an inverse routine is used to calculate a global temperature offset using the difference between modelled and observed benthic oxygen isotope abundance, implying that modelled and observed are per definition in agreement. In our new model set-up, the isotopic content of the ice-sheets is still tracked, but now the global mean temperature anomaly from the climate matrix is used to determine a deep-water temperature anomaly (ΔT_{dw}), and hence a modelled value for benthic $\delta^{18}O$. This deep-water temperature anomaly is calculated from the modelled mean annual surface temperature anomaly over the ocean following the approach by de Boer et al. (2014), using a 4,000-year running average and a scaling factor of 0.25. As opposed to the approach by de Boer et al. (2014), where an inverse method was used to match modelled

benthic $\delta^{18}O$ to an externally prescribed record, modelled $\delta^{18}O$ can now be independently compared to such a record in order to test the performance of the matrix method.

We compared our modelled benthic oxygen isotope abundance and the relative contributions to this signal by sea-water heavy oxygen enrichment and deep-water temperature change to data by Shakun et al. (2015), who analysed 49 ODP drilling locations where both surface-dwelling planktonic and benthic foraminiferal oxygen isotope abundance data were available, thereby allowing them to make a data-based decoupling of the contributions from ice volume and deep-water temperature to the benthic oxygen isotope signal. This model-data comparison is shown in Fig. 11. As can be seen, the results from the LGM benchmark experiment are in good agreement with the data, similar to the default ANICE model. The drop in benthic $\delta^{18}O$ at LGM of about 1.7 ‰ is reproduced comparably well by both the inverse method-forced model by de Boer et al. (2014) and the new matrix method-forced model set-up. The contribution from the change in deep-water temperature is slightly smaller in the new model set-up, though still in good agreement with the calculated global mean offset of 2 to 3 K at LGM. The new model set-up fails to reproduce the strong drop in benthic $\delta^{18}O$ during the inception of the glacial cycle, "catching up" only around 75 kyr.

3.4 Ice core temperature reconstructions

Shown in Fig. 12 are the modelled mean annual surface temperature anomalies over the Antarctic and Greenland ice sheets for the simulation with the default ANICE version and for the LGC benchmark experiment, compared to the EPICA Dome C reconstruction by Jouzel et al. (2007), and a stack of the GISP2 reconstruction by Alley (2000) and the NGRIP reconstruction by Kindler et al. (2014). As can be seen, both model versions agree well with each other and reasonably well with the Greenland isotope-based reconstructions (Alley, 2000; Kindler et al., 2014) regarding Greenland surface temperature anomalies. The Greenland records have been smoothed with a 4 ky running mean to filter out Dansgaard-Oeschger events, which are not present in our model forcing or climate reference runs and are also not included as feedback mechanisms in our model physics. Regarding Antarctic surface temperature anomalies, the new model set-up agrees particularly well with the EPICA isotope-based reconstruction (Jouzel et al., 2007), showing almost no significant deviations except for the first 20 kyr of the inception, where the model fails to reproduce the observed rapid cooling.

Deleted: GISP2 and NGRIP

Deleted: when neglecting the strong negative excursions during Dansgaard-Oeschger events

4 Conclusions

We have presented and evaluated a hybrid ice-sheet-climate model set-up that combines results from pre-calculated GCM simulations to force an ice-sheet model. Using the matrix method of GCM-ISM coupling, the impacts upon global climate of changes in atmospheric CO_2 concentration and global ice distribution are treated separately to construct a time-continuous climate forcing.

As a benchmark experiment, we used this new model set-up to simulate the entire last glacial cycle. Computational efficiency is such that this simulation could be performed within roughly 12 hours on a consumer-grade system. When compared with the default ANICE version by de Boer et al. (2014), the new model set-up performed better in simulating the volumes of the continental ice-sheets and their geographical position, and comparably well at simulating global mean deep-water temperature and isotopic content. The improved performance in terms of geographical position is likely a result of the improved dynamically driven changes in precipitation as solved by the GCM. Niu et al. (2017) showed that forcing the PISM ice-sheet model with output from several different GCM simulations of LGM from PMIP3, all of which were prescribed the same initial ice-sheets, resulted in a wide range of ice-sheet sizes at LGM (50 to 150 m SLE). This illustrates that, even though the ice-sheet prescribed to the GCM leaves a clear local "fingerprint" in the resulting climate, especially in the simulated temperature, this is by no means a guarantee that forcing an ice-sheet model with that climate will reproduce an ice-sheet that resembles the ice-sheet in the boundary conditions.

Modelled temperature anomalies over Greenland and Antarctica agree well with ice-core isotope-based reconstructions. When accounting for uncertainty in the applied forcing and model parameters, the simulated volume of the four major continental ice-sheets (excluding contributions from smaller ice caps, glaciers, thermal expansion and ocean area changes) at LGM amounted to 97 ± 11 m sea-level equivalent (± 2σ from the ensemble of simulations from the sensitivity analysis).

Deleted: 6

During the first 20 kyr of the inception, the model fails to reproduce the rapid drop in temperature and increase in ice volume visible in both benthic oxygen isotope records and ice-core isotope-based temperature reconstructions, implying that pCO_2 forcing alone is not sufficient to explain these observations without including some additional non-linear feedback processes. This is in line with results from other studies; studies like van de Wal et al. (2011) and de Boer et al. (2014) were able to reproduce the rapid cooling by using a forcing, such as a benthic oxygen isotope stack, that already incorporated the rapid decrease during the initial phase of the glacial cycle, whereas Bintanja and van de Wal (2008) and Niu et al. (2017) were unable to reproduce the rapid ice growth with pCO_2 forcing alone.

The effects of a growing ice-sheet on local and regional temperature are accounted for in the model through the resulting changes in albedo, but non-linear and non-local effects remain difficult to capture. Abe-Ouchi et al. (2013) constructed a model set-up similar to the matrix method presented here, but with more dimensions and corresponding GCM snapshots added to the matrix to decouple the different processes affecting temperature more explicitly: pCO_2, albedo, altitude and atmospheric stationary waves. Although their modelled ice-sheets at LGM do not match geomorphological reconstructions as well as the results presented here, they do report a stronger increase in ice volume during the inception. Expanding our climate matrix along the lines of their approach to more accurately describe the interplay between ice and climate for smaller ice-sheets could therefore potentially solve some of the repeatedly observed discrepancy between sea-level records and benthic $\delta^{18}O$ records on the one hand, and pCO_2 and temperature records on the other hand.

Deleted: However, several processes that would influence this effect are currently not included.

Other processes not accounted for in the albedo-based parameteristion of our climate matrix include glacial-interglacial changes in sea ice cover and changes in land albedo caused by changing vegetation. Including these feedback processes in the model could improve model performance in terms of the quantitative relation between pCO_2 and ice volume.

Deleted: G

Deleted: , though smaller than the changes in land ice cover, would have a strong influence on this process. Since ANICE does not model sea ice, this effect is not accounted for in the model.

Deleted: C

Deleted: , although of a smaller magnitude, are likewise not accounted for

5 Code and data availability

NetCDF files containing output data from the benchmark simulation (ice thickness, bedrock topography, mean annual temperature, annual precipitation, albedo and surface mass balance) are available as online supplementary material at doi: 10.5194/gmd-2018-145supplement, or directly at https://zenodo.org/record/1288386.

The source code of ANICE2.1, including the new matrix method, is available online at doi: 10.5194/gmd-2018-145code, or directly at https://zenodo.org/record/1299522. Note that the model code can be compiled but cannot be run without input data describing present-day climate and topography, initial ice thickness and topography and GCM output files constituting the climate matrix. For any questions regarding ANICE, please contact c.j.berends@uu.nl.

The output of the HadCM3 experiments which we used to construct the climate matrix can be obtained from Paul Valdes at the University of Bristol (P.J.Valdes@bristol.ac.uk).

6 Acknowledgements

The Ministry of Education, Culture and Science (OCW), in the Netherlands, provided financial support for this study via the program of the Netherlands Earth System Science Centre (NESSC). B. de Boer is funded by NWO Earth and Life Sciences (ALW), project 863.15.019. This work was sponsored by NWO Exact and Natural Sciences for the use of supercomputer facilities. Model runs were performed on the LISA Computer Cluster, we would like to acknowledge SurfSARA Computing and Networking Services for their support. Special thanks go to Paul Valdes for sharing the data from his HadCM3 simulations with us.

7 Appendix A: Mass balance

In the ANICE version used by de Boer et al. (2014), the entire mass balance module is forced by a global temperature offset, calculated from a prescribed $\delta^{18}O$ value and modelled global ice volume using the inverse routine by de Boer et al. (2013). This temperature offset, combined with a constant lapse-rate orography correction to account for changing ice thickness, is used to calculate a new monthly surface temperature field in every model time-step:

$$T(x,y) = T_{ref}(x,y) + dT_{glob} + \lambda\left(h(x,y) - h_{ref}(x,y)\right). \quad \text{(A1)}$$

Thus, the applied temperature T at horizontal location x, y is calculated at every model time step from the ERA-40 reference temperature T_{ref}, the global temperature offset dT_{glob} and the difference between the model orography h and the reference orography h_{ref}, multiplied by the constant lapse-rate λ of -8 K/km. For Greenland and Antarctica, the applied precipitation P is then calculated by correcting the monthly present-day reference value P_{ref} based on the difference between applied and reference temperature (Jouzel and Merlivat, 1984; Huybrechts, 1992):

$$P(x,y) = P_{ref}(x,y) \cdot 1.0266^{\left(T(x,y) - T_{ref}(x,y)\right)}. \quad \text{(A2)}$$

When simulating entire glacial cycles, the changes in ice-sheet geometry over North America and Eurasia are of a much larger scale then those over Greenland and Antarctica. In order to recreate the hypothesized westward growth of those ice-sheets during glacial inception, caused by orographic forcing of precipitation as moist wind blows up the slope of the ice-sheet and releases its moisture content, the precipitation model by Roe and Lindzen (2001) and Roe (2002) is used to calculate monthly precipitation values over these regions:

Deleted: 2, 2003

$$P(x,y) = P_{ref}(x,y)\frac{P_{Roe}(x,y)}{P_{Roe_{ref}}(x,y)}, \quad \text{(A3)}$$

$$dP_{Roe}(x,y) = e_{sat}(x,y)\, max\left(0,(a + bw'_{vv})\right) f(w'_{vv}) dw'_{vv}. \quad \text{(A4)}$$

$$e_{sat}(x,y) = e_0 \cdot e^{\left(\frac{c_1(T(x,y)-T_0)}{c_2+T(x,y)-T_0}\right)}, \quad \text{(A5)}$$

$$f(w'_{vv}) = \frac{1}{N} e^{\left(-\left(\frac{w'_{vv}-w_0}{\alpha}\right)^2\right)}, \quad \text{(A6)}$$

$$w_{vv}(x,y) = max\left(0, W_x(x,y)\frac{\partial h(x,y)}{\partial x} + W_y(x,y)\frac{\partial h(x,y)}{\partial y}\right). \quad \text{(A7)}$$

Here, e_{sat} is the saturation vapor pressure at the surface, which is a good proxy for the moisture content of the overlying air column. It is described by the Clausius-Clapeyron in Eq. A5 using the monthly mean surface temperature T, where e_0 = 6.112 mbar, c_1 = 17.67 and c_2 = 243.5 K. The vertical wind velocity w_{vv} is calculated from the 850 Hpa wind and the surface gradient according to Eq. A7. The precipitation P_{Roe} is related to vertical wind velocity w_{vv} through a probability distribution $f(w'_{vv})dw'_{vv}$, which is the probability that w_{vv} lies between w'_{vv} and $w'_{vv} + dw'_{vv}$, according to Eq. A6, where N is a

normalisation factor and $\alpha = 1.15$ cm s^{-1} is the measure of variability (Roe, 2002) in the vertical wind velocity. The precipitation P_{Roe} is given by Eq. A4, where the constants a = 2.5 · 10^{-11} kg^{-1} s^2 m and b = 5.9 · 10^{-9} s^3 kg were obtained by tuning to observations of Greenland (Roe, 2002). Eq. A4 is solved analytically using error functions (Roe and Lindzen, 2001).

Both w_{vv} and e_{sat} are calculated for both the reference state, using the reference temperature and orography fields, and for the model state, using the values at that model time step. The relative difference between the two modelled precipitation fields resulting from Eq. A4 is applied as an anomaly to the reference precipitation field to yield the applied precipitation field as described by Eq. A3.

Deleted: a = 2e-11 m^{2}kg^{-1}s; b = 5.9e-9 m kg^{-1}s^2; c_1 = 17.67; c_2 = 243.5 K; $E_{sat,0}$ = 611.2 Pa; α = 100 s m^{-1}, T_0 = 273 K. Here, the spatially variable field x_0 describes the change in upslope wind forcing calculated from the projected directional wind fields W_x and W_y and the local orographic slopes $\partial h/\partial x$ and $\partial h/\partial y$. The spatially variable field e_{sat} describes the saturation pressure as a function of local temperature.

Deleted: as described by Eq. A3

Figures A1 and A2 show the mean annual temperature and total annual precipitation fields at present-day and LGM respectively, resulting from applying these two methods to the initial ERA-40 temperature and precipitation fields, using the difference between the reference ERA-40 orography and the modelled orography at present-day and LGM.

The monthly surface mass balance is calculated from the applied surface temperature and precipitation fields and the prescribed incoming radiation at the top of the atmosphere following Laskar et al. (2004). Monthly values for accumulation, refreezing and ablation are calculated separately and added. First, the snow fraction of precipitation is calculated according to the parameterisation by Ohmura (1999):

$$f_{snow}(x,y) = \frac{1-0.796\cdot\tan^{-1}\left(\frac{T(x,y)-T_0}{3.5}\right)}{2}, \quad \text{(A7)}$$

where the spatially variable monthly snow fraction f_{snow} is defined as a function of 2-m air temperature. Monthly accumulation is simple the product of this fraction and monthly precipitation:

$$Acc(x,y) = P(x,y)\cdot f_{snow}(x,y). \quad \text{(A8)}$$

Local monthly ablation Abl is parameterised as a function of the 2-m air temperature T_{ano}, albedo α and incoming solar radiation at the top of the atmosphere Q_{TOA}, following the approach by Bintanja et al. (2002):

$$Abl(x,y) = c_1(T(x,y) - 273.15) + c_2\left(Q_{TOA}(x,y)\cdot\left(1-\alpha(x,y)\right)\right) - c_3, \quad \text{(A9)}$$

with c_1 = 0.0788 m y^{-1} K^{-1}, c_2 = 0.004 m^3 J^{-1} and c_3 a tuning parameter different for each individual ice-sheet (tuned values listed in Table 1).

The local monthly refreezing *Refr* is calculated from the available liquid water content L_w (the sum of liquid precipitation and ablation) and the superimposed water content L_{sup}, following the approach by Huybrechts and de Wolde (1999) and Janssens and Huybrechts (2000):

$$L_w(x,y) = P(x,y) \cdot \big(1 - f_{snow}(x,y)\big) + Abl(x,y), \quad \text{(A10)}$$

$$L_{sup}(x,y) = 0.012 \cdot \max\big(0, T_0 - T(x,y)\big), \quad \text{(A11)}$$

$$Refr(x,y) = \min\Big(L_w(x,y), L_{sup}(x,y), P(x,y)\Big). \quad \text{(A12)}$$

The surface mass balance *SMB* that will be used by the ice-sheet model is calculated as the sum of the accumulation *Acc*, the refreezing *Refr* and the ablation *Abl*:

$$SMB(x,y) = Acc(x,y) + Refr(x,y) - Abl(x,y). \quad \text{(A13)}$$

References

Abe-Ouchi, A., Saito, F., Kawamura, K., Raymo, M. E., Okuno, J., Takahashi, K. and Blatter, H.: Insolation-driven 100,000-year glacial cycles and hysteresis of ice-sheet volume, Nature Letters 500, 190-194, 2013.

Alley, R. B.: The Younger Dryas cold interval as viewed from central Greenland, Quaternary Science Reviews 19, 213-226, 2000.

Annan, J. D. and Hargreaves, J. C.: A new global reconstruction of temperature changes at the Last Glacial Maximum, Climate of the Past 9, 367-376, 2013.

Bamber, J. L., Riva, R. E. M., Vermeersen, B. L. A., and LeBrocq, A. M.: Reassessment of the potential sea-level rise from a collapse of the West Antarctic Ice Sheet, Science 324, 901-903, 2009.

Bintanja, R., van de Wal, R. S. W., and Oerlemans, J.: Global ice volume variations through the last glacial cycle simulated by a 3-D ice-dynamical model, Quaternary International 95-96, 11-23, 2002.

Bintanja, R., van de Wal, R., and Oerlemans, J.: Modelled atmospheric temperatures and global sea levels over the past million years, Nature 437, 125-128, 2005.

Bintanja, R. and van de Wal, R. S. W.: North American ice-sheet dynamics and the onset of 100,000-year glacial cycles, Nature 454, 869-872, 2008.

Braconnot, P., Otto-Bliesner, B., Harrison, S., Joussaume, S., Peterchmitt, J.-Y., Abe-Ouchi, A., Crucifix, M., Driesschaert, E., Fichefet, T., Hewitt, C. D., Kageyama, M., Kitoh, A., Laîné, A., Loutre, M.-F., Marti, O., Merkel, U., Ramstein, G., Valdes,

P. J., Weber, S. L., Yu, Y., and Zhao, Y.: Results of PMIP2 coupled simulations of the Mid-Holocene and Last Glacial Maximum - Part 1: experiments and large-scale features, Climate of the Past 3, 261-277, 2007.

Bradley, S. L., Reerink, T. J., van de Wal, R. S. W., and Helsen, M. M.: Simulation of the Greenland Ice sheet over two glacial cycles: Investigating a sub-ice shelf melt parameterisation and relative sea level forcing in an ice sheet-ice shelf model, Climate of the Past 14, 619-635, 2018.

Charbit, S., Ritz, C., and Ramstein, G.: Simulations of Northern Hemisphere ice-sheet retreat: sensitivity to physical mechanisms involved during the Last Deglaciation, Quaternary Science Reviews, 21, 243–265, 2002.

Charbit, S., Kageyama, M., Roche, D., Ritz, C., and Ramstein, G.: Investigating the mechanisms leading to the deglaciation of past continental northern hemisphere ice sheets with the CLIMBER–GREMLINS coupled model, Global and Planetary Change, 48, 253–273, 2005.

Charbit, S., Ritz, C., Philippon, G., Peyaud, V., and Kageyama, M.: Numerical reconstructions of the Northern Hemisphere ice sheets through the last glacial-interglacial cycle, Climate of the Past, 3, 15–37, 2007.

Church, J. A., Clark, P. U., Cazenave, A., Gregory, J. M., Jevrejeva, S., Levermann, A., Merrifield, M. A., Milne, G. A., Nerem, R. S., Nunn, P. D., Payne, A. J., Pfeffer, W. T., Stammer, D. and Unnikrishnan, A. S.: Sea-Level Change, Climate Change 2013: The Physical Science Basis. Contribution of Working Group 1 to the Fifth Assessment Report of the Intergovernmental Panel on Climate Change, 2013.

Dahl-Jensen, D., Mosegaard, K., Gundestrup, N., Clow, G. D., Johnsen, S. J., Hansen, A. W., and Balling, N.: Past Temperatures Directly from the Greenland Ice Sheet, Science 282, 268-272, 1998.

de Boer, B., van de Wal., R. S. W., Bintanja, R., Lourens, L. J., Tuenter, E.: Cenozoic global ice-volume and temperature simulations with 1-D ice-sheet models forced by benthic d18O records, Annals of Glaciology 51, 23-33, 2010.

de Boer, B., van de Wal, R. S. W., Lourens, L. J., Bintanja, R., and Reerink, T. J.: A continuous simulation of global ice volume over the past 1 million years with 3-D ice-sheet models, Climate Dynamics 41, 1365-1384, 2013.

de Boer, B., Stocchi, P., and van de Wal, R. S.W.: A fully coupled 3-D ice-sheet-sea-level model: algorithm and applications, Geoscientific Model Development 7, 2141-2156, 2014.

de Boer, B., Dolan, A. M., Bernales, J., Gasson, E., Goelzer, H., Golledge, N. R., Sutter, J., Huybrechts, P., Lohmann, G., Rogozhina, I., Abe-Ouchi, A., Saito, F., and van de Wal, R. S. W.: Simulating the Antarctic ice sheet in the Late-Pliocene warm period: PLISMIP-ANT, an ice-sheet model intercomparison project, The Cryosphere 8, 5539-5588, 2015.

Dolan, A. M., Haywood, A. M., Lunt, D. J., Dowsett, H. J., Hunter, S. J., Lunt, D. J., and Pickering, S. J.: Sensitivity of Pliocene ice sheets to orbital forcing, Palaeogeography, Palaeoclimatology and Palaeoecology 309, 98-110, 2011.

Dolan, A. M., Haywood, A. M., Hunter, S. J., Tindall, J. C., Dowsett, H. J., Hill, D. J., and Pickering, S. J.: Modelling the enigmatic Late Pliocene Glacial Event - Marine Isotope Stage M2, Global and Planetary Change 128, 47-60, 2015.

Duplessy, J.-C., Labeyrie, L. and Waelbroeck, C.: Constraints on the ocean oxygen isotopic enrichment between the Last Glacial Maximum and the Holocene: Paleoceanographic implications, Quaternary Science Reviews 21, 315-330, 2002.

Dutton, A., Carlson, A. E., Long, A. J., Milne, G. A., Clark, P. U., DeConto, R. M., Horton, B. P., Rahmstorf, S., and Raymo, M. E.: Sea-level rise due to polar ice-sheet mass loss during past warm periods, Science 349, 153-163, 2015.

Ehlers, J. and Gibbard, P. L.: The extent and chronology of Cenozoic Global Glaciation, Quaternary International 164, 6-20, 2007.

Ganopolski, A., Calov, R., and Claussen, M.: Simulation of the last glacial cycle with a coupled climate ice-sheet model of intermediate complexity, Climate of the Past, 6, 229–244, 2010.

Gordon, C., Cooper, C., Senior, C. A., Banks, H., Gregory, J. M., Johns, T. C., Mitchell, J. F. B., and Wood, R. A.: The simulation of SST, sea ice extents and ocean heat transports in a version of the Hadley Centre coupled model without flux adjustments, Climate Dynamics 16, 147-168, 2000.

Gregory, J. M., Browne, O. J. H., Payne, A. J., Ridley, J. K. and Rutt, I. C.: Modelling large-scale ice-sheet-climate interactions following glacial inception, Climate of the Past 8, 1565-1580, 2012.

Haywood, A. M., Hill, D. J., Dolan, A. M., Otto-Bliesner, B., Bragg, F., Chan, W.-L., Chandler, M. A., Contoux, C., Dowsett, H. J., Jost, A., Kamae, Y., Lohmann, G., Lunt, D. J., Abe-Ouchi, A., Pickering, S. J., Ramstein, G., Rosenbloom, N. A., Salzmann, U., Sohl, L., Stepanek, C., Ueda, H., Yan, Q., and Zhang, Z.: Large-scale features of Pliocene climate: results from the Pliocene Model Intercomparison Project, Climate of the Past 9, 191-209, 2013.

Haywood, A. M. and Valdes, P. J.: Modelling Pliocene warmth: contribution of atmosphere, oceans and cryosphere, Earth and Planetary Science Letters 218, 363-377, 2003.

Helsen, M. M., van de Berg, W. J., van de Wal, R. S. W., van den Broeke, M. R. and Oerlemans, J.: Coupled regional climate-ice-sheet simulations show limited Greenland ice loss during the Eemian, Climate of the Past 9, 1773-1788, 2013.

Hewitt, C. D., Broccoli, A. J., Mitchell, J. F. B., Stouffer, R. J.: A coupled model study of the last glacial maximum: Was part of the North Atlantic relatively warm?, Geophysical Research Letters 28, 1571-1574, 2001.

Herrington, A. and Poulsen, C. J.: Terminating the Last Interglacial: The Role of Ice Sheet-Climate Feedbacks in a GCM Asynchronously Coupled to an Ice Sheet Model, Journal of Climate, 1871-1882, 2012.

Hughes, A. L. C., Gyllencreutz, R., Lohne, Ø., Mangerud, J. and Svendsen, J. I.: The last Eurasian ice sheets - a chronological database and time-slice reconstruction, DATED-1, Boreas 45, 1-45, 2016.

Huybrechts, P.: The Antarctic ice sheet and environmental change: a three-dimensional modelling study, Berichte zur Polarforschung 99, 1992.

Huybrechts, P.: Sea-level changes at the LGM from ice-fynamic reconstructions of the Greenland and Antarctic ice sheets during the glacial cycles, Quaternary Science Reviews 21, 203-231, 2002.

Huybrechts, P. and de Wolde, J.: The Dynamic Response of the Greenland and Antarctic Ice Sheets to Multiple-Century Climatic Warming, Journal of Climate 12, 2169-2188, 1999.

Jansen, E., Overpeck, J., Briffa, K.R., Duplessy, J.-C., Joos, F., Masson-Delmotte, V., Olago, D.O., Otto-Bliesner, B., Peltier, W.R., Rahmstorf, S., Ramesh, R., Raynaud, D., Rind, D.H., Solomina, O., Villalba, R., Zhang, D., 2007. Palaeoclimate. In: Solomon, S., Qin, D., Manning, M., Chen, Z., Marquis, M., Averyt, K.B., Tignor, M., Miller, H.L. (Eds.), Climate Change

2007: The Physical Science Basis. Contribution of Working Group I to the Fourth Assessment Report of the Intergovernmental panel on Climate Change. Cambridge University Press, Cambridge, UK, and New York, pp. 433–497.

Janssens, I. and Huybrechts, P.: The treatment of meltwater retention in mass-balance parameterizations of the Greenland ice sheet, Annals of Glaciology 31, 133-140, 2000.

Jouzel, J., Masson-Delmote, V., Cattani, O., Dreyfus, G., Falourd, S., Hoffmann, G., Minster, B., Nouet, J., Barnola, J. M., Chappellaz, J., Fischer, H., Gallet, J. C., Johnsen, S., Leuenberger, M., Loulergue, L., Luethi, D., Oerter, H., Parrenin, F., Raisbeck, G., Raynaud, D., Schilt, A., Schwander, J., Selmo, E., Souchez, R., Spahni, R., Stauffer, B., Steffensen, J. P., Stenni, B., Stocker, T. F., Tison, J. L., Werner, M., and Wolff, E. W.: Orbital and Millenioal Antarctic Climate Variability over the Past 800,000 Years, Science 317, 793-797, 2007.

Jouzel, J. and Merlivat, L.: Deuterium and Oxygen 18 in Precipitation: Modelling of the Isotopic Effects During Snow Formation, Journal of Geophysical Research 89, 11,749-11,757, 1984.

Kindler, P., Guillevic, M., Baumgartner, M., Schwander, J., Landais, A., and Leuenberger, M.: Temperature reconstruction from 10 to 120 kyr b2k from the NGRIP ice core, Clim. Past 10, 887-902, 2014.

Laskar, J., Robutel, P., Gastineau, M., Correia, A. C. M., and Levrard, B.: A long-term numerical solution for the insolation quantities of the Earth, Astronomy & Astrophysics 428, 261-285, 2004.

Lhomme, N. and Clarke, G. K. C.: Global budget of water isotopes inferred from polar ice sheets, Geophysical Research Letters 32, 2005.

Lisiecki, L. E. and Raymo, M. E.: A Pliocene-Pleistocene stack of 57 globally distributed benthic delta-18-O records, Paleoceanography 20, 2005.

Loulergue, L., Schilt, A., Spahni, R., Masson-Delmotte, V., Blunier, T., Lemieux, B., Barnola, J.-M., Raynaud, D., Stocker, T.F. and Chappellaz, J.: Orbital and millennial-scale features of atmospheric CH4 over the past 800,000 years, Nature 453, 383–386, 2008.

Lūthi, D., Le Floch, M., Bereiter, B., Blunier, T., Barnola, J.-M., Siegenthaler, U., Raynaud, D., Jouzel, J., Fisher, H., Kawamura, K., and Stocker, T. F.: High-resolution carbon dioxide concentration record 650,000-800,000 years before present, Nature Letters 452, 379-382, 2008.

Ma, Y., Gagliardini, O., Ritz, C., Gillet-Chaulet, F., Durand, G., Montagnat, M.: Enhancement factors for grounded ice and ice shelves inferred from an anisotropic ice-flow model, Jour. Glac. 56, 805-812, 2010.

Marshall, S. J., Tarasov, L., Clarke, G. K., and Peltier, W. R.: Glaciological reconstruction of the Laurentide Ice Sheet: physical processes and modelling challenges, Canadian Journal of Earth Sciences, 37, 769–793, 2000.

Marshall, S. J., James, T. S., and Clarke, G. K.: North American ice sheet reconstructions at the Last Glacial Maximum, Quaternary Science Reviews, 21, 175–192, 2002.

Martin, M. A., Winkelmann, R., Haseloff, M., Albrecht, T., Bueler, E., Khroulev, C., Levermann, A.: The Potsdam Parallel Ice Sheet Model (PISM-PIK)–Part 2: Dynamic equilibrium simulation of the Antarctic ice sheet, The Cryosphere 5, 727–740, 2011.

Masson-Delmote, V., Jouzel, J., Landais, A., Stievenard, M., Johnsen, S. J., White, J. W. C., Werner, M., Sveinbjornsdottir, A., and Fuhrer, K.: GRIP Deuterium Excess Reveals Rapid and Orbital-Scale Changes in Greenland Moisture Origin, Science 309, 118-122, 2005.

Niu, L., Lohmann, G., Hinck, S. and Gowan, E. J.: Sensitivity of atmospheric forcing on Northern Hemisphere ice sheets during the last glacial-interglacial cycle using output from PMIP3, Climate of the Past Discussions, 2017.

Ohmura, A.: Precipitation, accumulation and mass balance of the Greenland ice sheet, Zeitschrift fur Gletscherkunde und Glazialgeologie 35, 1-20, 1999.

Peltier, W. R.: Global Glacial Isostasy and the Surface of the Ice-Age Earth: The ICE-5G (VM2) Model and GRACE, Annu. Rev. Earth Planet. Sci. 32, 111-149, 2004.

Petit, J.R., Jouzel, J., Raynaud, D., Barkov, N.I., Barnola, J.-M., Basile, I., Bender, M., Chappellaz, J., Davis, J., Delaygue, G., Delmotte, M., Kotlyakov, V.M., Legrand, M., Lipenkov, V., Lorius, C., Pepin, L., Ritz, C., Saltzman and E., Stievenard, M.: Climate and atmospheric history of the past 420 000 years from the Vostok Ice Core, Antarctica. Nature 399, 429–436, 1999.

Pollard, D.: A retrospective look at coupled ice sheet-climate modeiing, Climatic Change 100, 173-194, 2010.

Pollard, D. and DeConto, R. M.: Modelling West Antarctic ice sheet growth and collapse through the past five million years, Nature 458, 329-332, 2009.

Pollard, D., Kump, L. R., and Zachos, J. C.: Interactions between carbon dioxide, climate, weathering, and the Antarctic ice sheet in the earliest Oligocene, Global and Planetary Change 111, 258-267, 2013.

Roe, G. H.: Modelling precipitation over ice sheets: an assessment using Greenland, Journal of Glaciology 48, 70-80, 2002.

Roe, G. H. and Lindzen, R. S.: The Mutual Interaction between Continental-Scale Ice Sheets and Atmospheric Stationary Waves, Journal of Climate 14, 1450-1465, 2001.

Rohling, E. J., Grant, K., Bolshaw, M., Roberts, A. P., Siddall, M., Hemleben, Ch. and Kucera, M.: Antarctic temperature and global sea level closely coupled over the past five glacial cycles, Nature Geosciences Letters 2, 500-504, 2009.

Shakun, J. D., Lea, D. W., Lisiecki, L. E., and Raymo, M. E.: An 800-kyr record of global surface ocean d18O and implications for ice volume-temperature coupling, Earth and Planetary Science Letters 426, 58-68, 2015.

Singarayer, J. S. and Valdes, P. J.: High-latitude climate sensitivty to ice-sheet forcing over the last 120 kyr, Quaternary Science Reviews 29, 43-55, 2010.

Solomon, S., Qin, D., Manning, M., Chen, Z., Marquis, M., and Averyt, K. B.: Climate Change 2007: the physical science basis. Contribution Of Working Group I To The Fourth Assessment Report Of The Intergovernmental Panel On Climate Change, 2007.

Stap, L. B., van de Wal, R. S. W., de Boer, B., Bintanja, R. and Lourens, L. J.: Interaction of ice sheets and climate during the past 800 000 years, Climate of the Past 10, 2135-2152, 2014.

Stap, L. B., de Boer, B., Ziegler, M., Bintanja, R., Lourens, L. J. and van de Wal, R. S. W.: CO2 over the past 5 million years: Continuous simulation and new d11B-based proxy data, Earth and Planetary Science Letters 439, 1-10, 2016.

Tan, N., Ramstein, G., Dumas, C., Contoux, C., Ladant, J.-B., Sepulchre, P., Zhang, Z., and de Schepper, S.: Exploring the MIS M2 glaciation occurring during a warm and high atmospheric CO2 Pliocene background climate, Earth and Planetary Science Letters , 266-276, 2017.

Tarasov, L. and Peltier, W. R.: A geophysically constrained large ensemble analysis of the deglacial history of the North American ice-sheet complex, Quaternary Science Reviews 23, 359-388, 2004.

Thompson, W. G. and Goldstein, Steven L.: A radiometric calibration of the SPECMAP timescale, Quaternary Science Reviews 25, 3207-3215, 2006.

Uppala, S. M., Kallberg, P. W., Simmons, A. J., Andrae, U., da Costa Bechtold, V., Fiorino, M., Gibson, J. K., Haseler, J., Hernandez, A., Kelly, G. A., Li, X., Onogi, K., Saarinen, S., Sokka, N., Allan, R. P., Andersson, E., Arpe, K., Balmaseda, M. A., Beljaars, A. C. M., van de Berg, L., Bidlot, J., Bormann, N., Caires, S., Chevallier, F., Dethof, A., Dragosavac, M., Fisher, M., Fuentes, M., Hagemann, S., Holm, E., Hoskins, B. J., Isaksen, L., Janssen, P. A. E. M., Jenne, R., McNally, A. P., Mahfouf, J.-F., Morcrette, J.-J., Rayner, N. A., Saunders, R. W., Simon, P., Sterl, A., Trenberth, K. E., Untch, A., Vasiljevic, D., Viterbo, P., and Woollen, J.: The ERA-40 re-analysis, Quarterly Journal of the Royal Meteorological Society 131, 2961-3012, 2005.

Valdes, P. J., Armstrong, E., Badger, M. P. S., Bradshaw, C. D., Bragg, F., Crucifix, M., Davies-Barnard, T., Day, J. J., Farnsworth, A., Gordon, C., Hopcroft, P. O., Kennedy, A. T., Lord, N. S., Lunt, D. J., Marzocchi, A., Parry, L. M., Pope, V., Roberts, W. H. G., Stone, E. J., Gregory, J. L. T. and Williams, Jonny H. T.: The BRIDGE HadCM3 family of climate models: HadCM3@Bristol v1.0, Geosci. Mod. Dev. 10, 3715-3743, 2017.

Winkelmann, R., Martin. M. A., Haseloff, M., Albrecht, T., Bueler, E., Khroulev, C., Levermann, A.: The Potsdam Parallel Ice Sheet Model (PISM-PIK)—part 1: Model description, The Cryosphere 5, 715–726, 2011.

van de Wal, R. S. W., de Boer, B., Lourens, L. J., Köhler, P. and Bintanja, R.: Reconstruction of a continuous high-resolution CO_2 record over the past 20 million years, Climate of the Past 7, 1459-1469, 2011.

Zweck, C. and Huybrechts, P.: Modeling of the northern hemisphere ice sheets during the last glacial cycle and glaciological sensitivity, Jour. of Geophys. Res. 110, 2005.

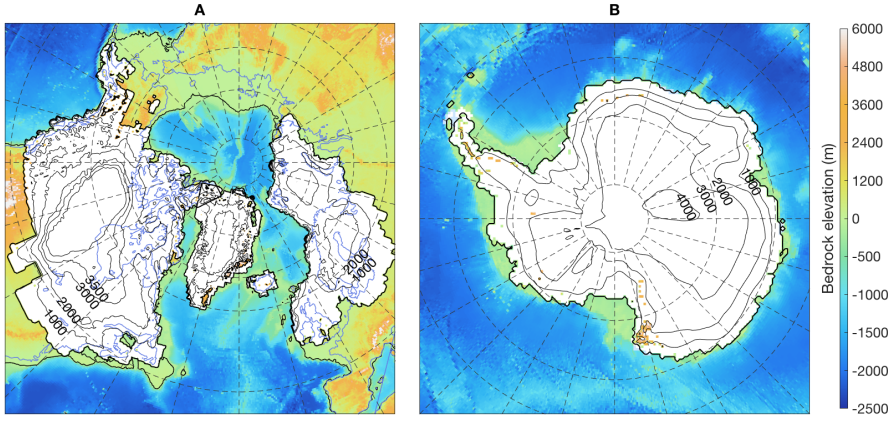

Figure 1: LGM ice thickness distributions from the ICE-5G reconstruction (Peltier, 2004) for A) the Northern hemisphere and B) Antarctica. Contour lines for the Northern Hemisphere show ice thickness, contour lines for Antarctica show surface elevation. Bedrock elevtion where not covered by ice shown by colors, present-day shorelines shown in blue.

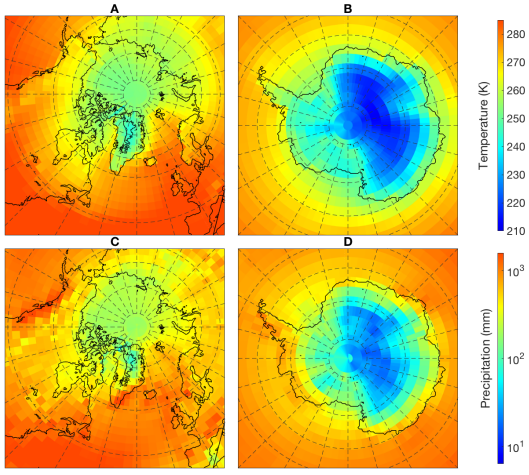

Figure 1: Annual mean 2m temperature for the Northern Hemisphere (A) and Antarctica (B) and total annual precipitation (C and D), calculated with HadCM3 in the PI_Control experiment (Singarayer and Valdes, 2010).

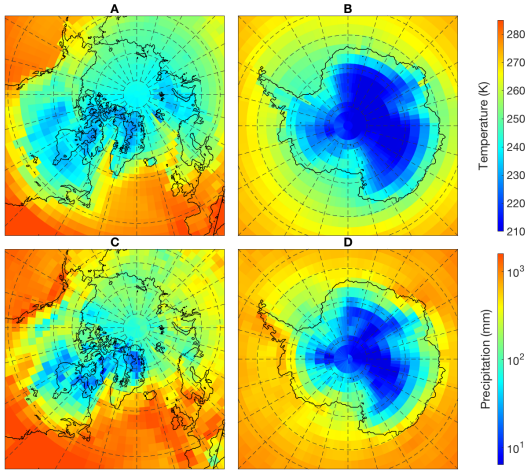

Figure 3: Annual mean 2m temperature for the Northern Hemisphere (A) and Antarctica (B) and total annual precipitation (C and D), calculated with HadCM3 in the LGM experiment (Singarayer and Valdes, 2010).

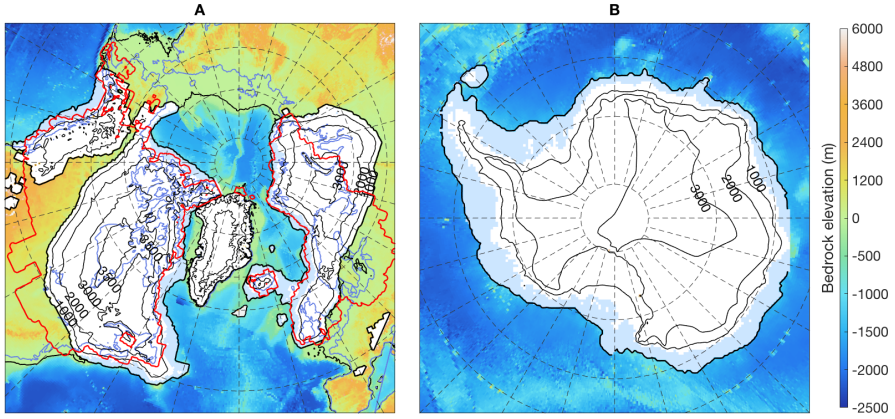

Figure 4: Ice-sheets (white) and shelves (light blue) at LGM over A) the Northern Hemisphere and B) Antarctica, as simulated with the default ANICE version from de Boer et al. (2014). Contour lines for the Northern Hemisphere show ice thickness, contour lines for Antarctica show surface elevation. Bedrock elevtion where not covered by ice shown by colors, present-day shorelines shown in blue, ICE-5G ice margin shown in red.

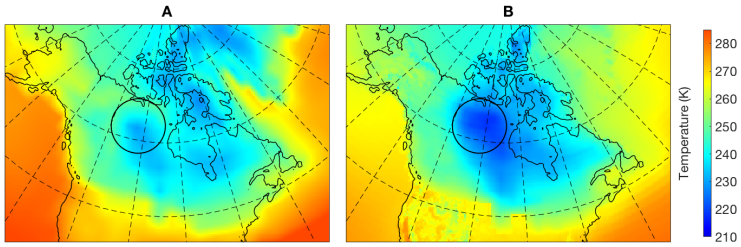

Figure 5: Mean annual surface temperature at LGM over North America as generated with HadCM3 by Singarayer and Valdes (2010) (A) versus the temperature field generated for these conditions using a constant lapse-rate approach (B). GCM temperatures are substantially higher over the main dome of the ice-sheet (area indicated by black circle).

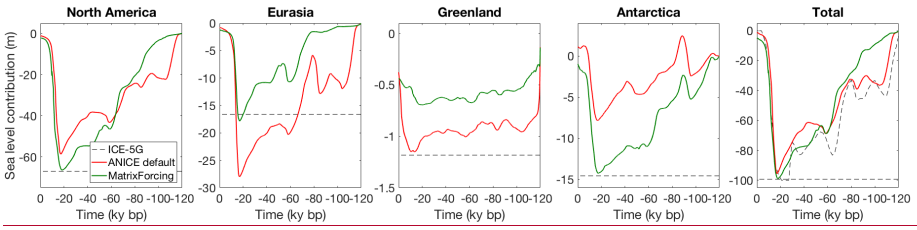

Figure 6: Global mean sea-level contributions over time for the four individual ice-sheets, as well as the global total, for the LGC benchmark experiment (green) and the default ANICE control run (red), compared to the ICE-5G sea-level at LGM (dashed line).

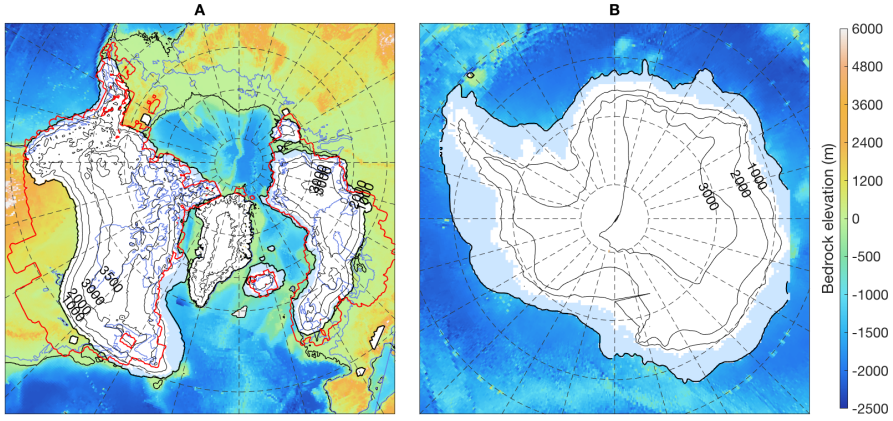

Figure 7: Ice-sheets (white) and shelves (light blue) at LGM over A) the Northern Hemisphere and B) Antarctica, as simulated with the new model set-up. Contour lines for the Northern Hemisphere show ice thickness, contour lines for Antarctica show surface elevation. Bedrock elevtion where not covered by ice shown by colors, present-day shorelines shown in blue, ICE-5G ice margin shown in red.

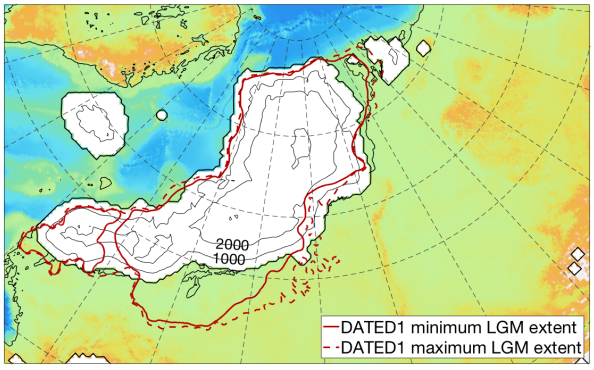

Figure 8: Comparison of the simulated Eurasian ice-sheet at LGM with the DATED-1 reconstruction (Hughes et al., 2016). Contour lines show ice thickness. The modelled ice-sheet has a volume of 17 m sea-level equivalent, in agreement with the 17 m of the ICE-5G reconstruction, whereas the DATED-1 ice-sheet is equivalent to 24 m sea-level.

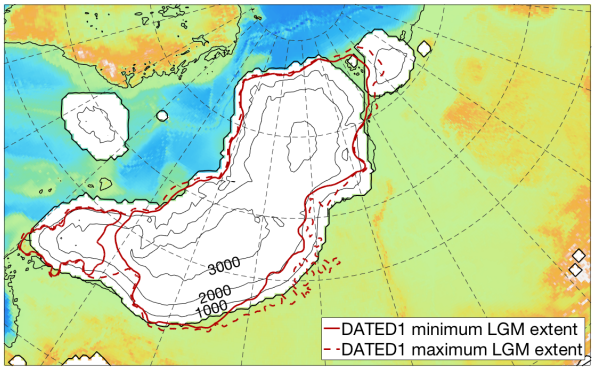

Figure 9: Comparison of the larger simulated Eurasian ice-sheet at LGM with the DATED-1 reconstruction (Hughes et al., 2016). Contour lines show ice thickness. The modelled ice-sheet has a volume of 24 m sea-level equivalent, in agreement with the DATED-1 ice-sheet.

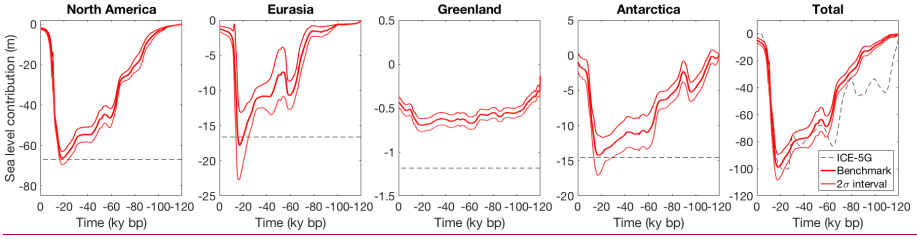

Figure 10: Modelled sea level contribution over time for all four individual ice-sheets, and the total sum. The ± 2σ confidence interval is shown for the ensemble of simulations from the sensitivity analysis.

Deleted: Dotted lines indicate upper and lower limits for prescribed CO_2 forcing (blue), ablation tuning parameter (green) and SIA/SSA flow enhancement factor ratio (purple)

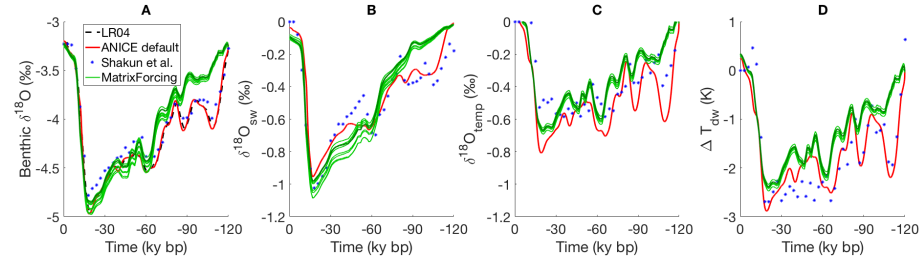

Figure 11: A) modelled benthic oxygen isotope abundance from the default ANICE model (de Boer et al., 2014) and the LGM benchmark experiment compared to different datasets (LR04, Shakun et al. (2015). B) $\delta^{18}O$ of seawater due to depletion of heavy isotopes. C) contribution to benthic oxygen isotope abundance due to changes in deep-water temperature. D) derived deep-water temperature anomaly.

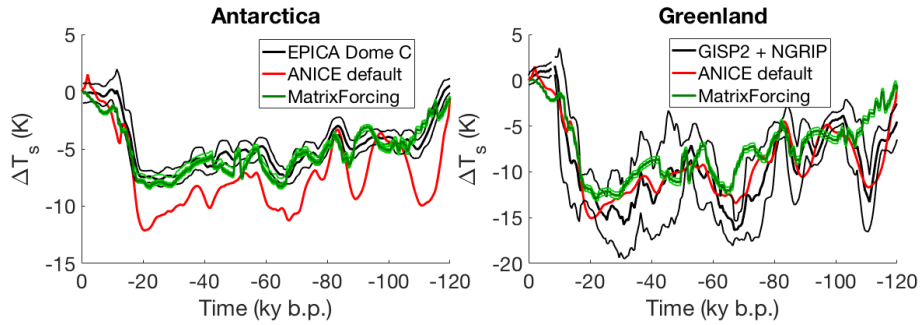

Figure 12: Modelled versus reconstructed temperature anomaly for Antarctica (EPICA Dome C; Jouzel et al., 2007) and Greenland (GISP2; Alley, 2000; NGRIP; Kindler et al., 2014).

Table 1: Tuned values of the ablation parameter c_3 as used in Eq. A9.

Region	North America	Eurasia	Greenland	Antarctica
c_3 **(m/y)**	0.14	0.23	0.19	0.14

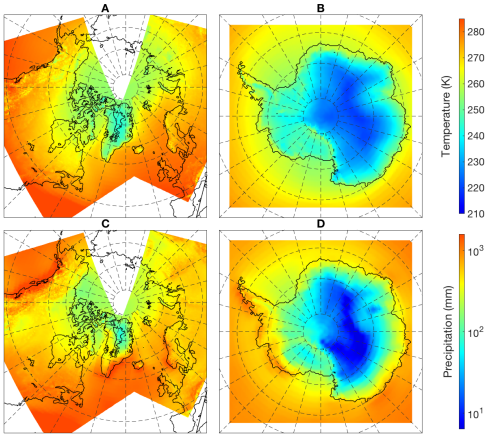

Figure A1: Annual mean 2m temperature for the Northern Hemisphere (A) and Antarctica (B) and total annual precipitation (C and D), resulting from applying the constant lapse-rate temperature change and the Roe precipitation model to the ERA-40 climate fields.

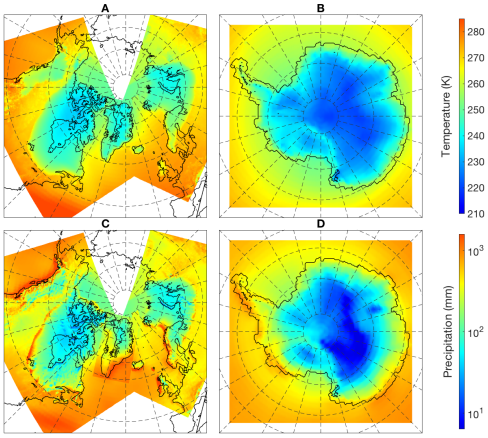

Figure A2: Annual mean 2m temperature for the Northern Hemisphere (A) and Antarctica (B) and total annual precipitation (C and D), resulting from applying the constant lapse-rate temperature change plus global offset and the Roe precipitation model to the ERA-40 climate fields and the ANICE LGM ice-sheets.